Activation of airway epithelial bitter taste receptors by *Pseudomonas aeruginosa* quinolones modulates calcium, cyclic-AMP, and nitric oxide signaling

Received for publication, November 26, 2017, and in revised form, April 17, 2018 Published, Papers in Press, May 10, 2018, DOI 10.1074/jbc.RA117.001005

Jenna R. Freund[‡], Corrine J. Mansfield[§], Laurel J. Doghramji[‡], Nithin D. Adappa[‡], James N. Palmer[‡], David W. Kennedy[‡], Danielle R. Reed[§], Peihua Jiang[§], and Robert J. Lee[‡¶1]

From the Departments of [‡]Otorhinolaryngology–Head and Neck Surgery and [¶]Physiology, University of Pennsylvania Perelman School of Medicine, Philadelphia, Pennsylvania 19104 and the [§]Monell Chemical Senses Center, Philadelphia, Pennsylvania 19104

Edited by Peter Cresswell

Bitter taste receptors (taste family 2 bitter receptor proteins; T2Rs), discovered in many tissues outside the tongue, have recently become potential therapeutic targets. We have shown previously that airway epithelial cells express several T2Rs that activate innate immune responses that may be important for treatment of airway diseases such as chronic rhinosinusitis. It is imperative to more clearly understand what compounds activate airway T2Rs as well as their full range of functions. T2R isoforms in airway motile cilia (T2R4, -14, -16, and -38) produce bactericidal levels of nitric oxide (NO) that also increase ciliary beating, promoting clearance of mucus and trapped pathogens. Bacterial quorum-sensing acyl-homoserine lactones activate T2Rs and stimulate these responses in primary airway cells. Quinolones are another type of quorum-sensing molecule used by *Pseudomonas aeruginosa*. To elucidate whether bacterial quinolones activate airway T2Rs, we analyzed calcium, cAMP, and NO dynamics using a combination of fluorescent indicator dyes and FRET-based protein biosensors. T2R-transfected HEK293T cells, several lung epithelial cell lines, and primary sinonasal cells grown and differentiated at the air–liquid interface were tested with 2-heptyl-3-hydroxy-4-quinolone (known as *Pseudomonas* quinolone signal; PQS), 2,4-dihydroxyquinolone, and 4-hydroxy-2-heptylquinolone (HHQ). In HEK293T cells, PQS activated T2R4, -16, and -38, whereas HHQ activated T2R14. 2,4-Dihydroxyquinolone had no effect. PQS and HHQ increased calcium and decreased both baseline and stimulated cAMP levels in cultured and primary airway cells. In primary cells, PQS and HHQ activated levels of NO synthesis previously shown to be bactericidal. This study suggests that airway T2R-mediated immune responses are activated by bacterial quinolones as well as acyl-homoserine lactones.

This study was supported in part by National Institutes of Health Grants R03DC013862 and R01DC016309, Cystic Fibrosis Foundation Grant LEER16G0, and the Department of Otorhinolaryngology at the University of Pennsylvania (to R. J. L.). Genotyping of patient samples was supported by National Institutes of Health Grants P30DC011735 and S10OD018125 (to D. R. R.). The authors declare that they have no conflicts of interest with the contents of this article. The content is solely the responsibility of the authors and does not necessarily represent the official views of the National Institutes of Health.

This article contains Table S1 and Figs. S1–S8.

[1] To whom correspondence should be addressed: Dept. of Otorhinolaryngology–Head and Neck Surgery, Hospital of the University of Pennsylvania, Ravdin, 5th Fl., Ste. A, 3400 Spruce St., Philadelphia, PA 19104. Tel.: 215-573-9766; E-mail: rjl@pennmedicine.upenn.edu.

The immune system has been referred to as the "sixth sense" (1–5) because it detects invading pathogens similarly to the way the other five senses (touch, taste, smell, sight, and hearing) perceive the external environment. Fitting this viewpoint, we and others have demonstrated that the immune and taste systems both utilize some of the same chemosensory receptors. Bitter taste receptors (also known as a taste family 2 receptors, or T2Rs)[2] are G protein–coupled receptors (GPCRs) used by the tongue to detect compounds that are perceived as bitter (6, 7). There are 25 T2R isoforms on the human tongue, and many isoforms are also expressed in organs such as the brain, nose and sinuses, lung, and reproductive tract (6–10). The functions of these so-called "extraoral" taste receptors and their physiological ligands in many tissues are largely unknown, although they may be responsible for some off-target effects of many commonly used medications that taste bitter (*e.g.* aspirin) (11).

T2R38 is expressed in the motile cilia of cells of the upper airway (nose and sinuses), and it is activated in response to acyl-homoserine lactone (AHL) quorum-sensing molecules secreted by Gram-negative bacteria (12), including the common airway pathogen *Pseudomonas aeruginosa*. T2R38 activation causes an increase in intracellular free Ca^{2+} concentration ($[Ca^{2+}]_i$) that activates nitric-oxide synthase (NOS) to produce nitric oxide (NO) (9, 12–17). NO activates production of cGMP to activate protein kinase G, which increases ciliary beating and enhances mucociliary clearance, the major physical defense of the airway. The T2R-activated NO also directly diffuses into the airway surface liquid, where it has antibacterial effects (12, 18),

[2] The abbreviations used are: T2R, taste family 2 bitter receptor protein; 2FLI, 2-furoyl-LIGRLO-amide; AF, Alexa Fluor; AHL, acyl-homoserine lactone; ALI, air–liquid interface culture; AKAR, A-kinase activity reporter; AM, acetoxymethyl ester; ANOVA, analysis of variance; CF, cystic fibrosis; CFP, cyan fluorescent protein; CFTR, cystic fibrosis transmembrane conductance regulator; CKAR, C-kinase activity reporter; DAF-FM, 4-amino-5-metholamino-2′,7′-difluorofluorescein diacetate; DHQ, 2,4-dihydroxyquinolone, also known as 2,4-quinolinediol; FFA, flufenamic acid; GPCR, G-protein-coupled receptor; HBSS, Hanks' balanced salt solution; HHQ, 4-hydroxy-2-heptyl quinolone, sometimes referred to as 2-heptyl-4-quinoline; IBMX, isobutylmethylxanthine; IL, interleukin; IP_3, inositol trisphosphate; NA, numerical aperture; NOS, nitric-oxide synthase; PAR-2, protease-activated receptor 2; PDE, phosphodiesterase; PKA, protein kinase A; PLC, phospholipase; PMA, phorbol 12-myristate 13-acetate; PQS, *Pseudomonas* quinolone signal (2-heptyl-3-hydroxy-4-quinolone); PRR, pattern recognition receptor; PTC, phenylthiocarbamide; PTX, pertussis toxin; RNS, reactive nitrogen species; *TAS2R*, taste family 2 bitter receptor gene; YFP, yellow fluorescent protein.

probably through damage to bacterial cell walls and/or DNA (19, 20).

The relevance of T2R38 to immunity is supported by clinical data linking polymorphisms in the *TAS2R38* gene to sinonasal disease (16, 21). Patients homozygous for the AVI *TAS2R38* polymorphism, which results in nonfunctional T2R38 protein (22), are more susceptible to Gram-negative bacterial infection (12), have higher levels of sinonasal bacteria (23, 24) and biofilms (25), are at higher risk for chronic rhinosinusitis (26–29), and may have worse outcomes after endoscopic sinus surgery (30) compared with patients homozygous for the functional (PAV) allele of *TAS2R38*.

We subsequently identified other T2R isoforms, T2R4, T2R14, and T2R16, in sinonasal cilia (31, 32). These isoforms are also in bronchial cilia (10). Activation of these T2Rs in sinonasal cells by known bitter compounds produces similar Ca^{2+} and NO responses. We hypothesize that yet-unknown pathogen-produced products activate these other T2Rs in addition to AHL activation of T2R38. One such class of compounds may be quinolones, which are involved in quorum sensing in bacteria.

Quorum sensing involves detection of secreted compounds that provide information about population density, allowing coordination of behavior among single-celled organisms (33, 34). The Las and Rhl systems, which utilize secreted AHLs, are found in nearly all Gram-negative bacteria (33, 34) and regulate processes such as biofilm formation (35, 36). Another system exists in *P. aeruginosa*, the Pqs system, which involves enzymes that produce up to 50 different quinolones (34, 35, 37–39). Three quinolones, described below, have been implicated in bacterial virulence through activation of the LysR-type transcription factor PqsR, promoting biofilm formation and production of pyocyanin (38, 39), which impairs cilia function (40–42) and activates inflammation (43) in airway cells. We noticed that these quinolones have some structural similarities to the prototypical bitter compounds quinine and chloroquine (Fig. 1*a*), one of several quinolone antibiotics known to taste bitter (44). Quinine activates nine T2Rs (T2R4, -7, -10, -14, -39, -40, -43, -44, and -46), whereas chloroquine activates five T2Rs (T2R3, -7, -10, -14, and -39) (45–47).

The most well-studied *P. aeruginosa* quinolone is 2-heptyl-3-hydroxy-4-quinolone, commonly referred to as *Pseudomonas* quinolone signal (PQS) (37–39, 44). PQS (M_r 259.34) is produced in pre-biofilm laboratory *P. aeruginosa* cultures at up to 6–9 ng/μl (48), equating to ~23–35 μM. PQS may be involved in stress responses required for survival under harsh conditions (49) and/or aid in iron accumulation (50, 51). PQS also controls production of rhamnolipids, elastase, and pyocyanin (52, 53). Increased synthesis of PQS was reported in *P. aeruginosa* isolates during early (presymptomatic) colonization of cystic fibrosis (CF) patient lungs (54). Another study reported detection of PQS in sputum samples from *P. aeruginosa*-infected but not uninfected CF patients (55), suggesting that PQS detection may have specific relevance to CF lung infections. A recent study reported that swarming communities of *P. aeruginosa* may produce PQS at concentrations up to 150 μM in response to the antibiotic tobramycin (56), which has been frequently used to treat *P. aeruginosa* infections in CF (57).

Two other *P. aeruginosa*-derived quinolones, 4-hydroxy-2-heptylquinolone (HHQ) and 2,4-dihydroxyquinolone (DHQ) (Fig. 1*a*), may also function in quorum sensing. HHQ is an autoinducer (50, 58) and modulates swarming motility (59). DHQ is important for virulence in *C. elegans* models of *P. aeruginosa* infection (60). DHQ concentrations may reach 50–100 μM in cultures of the common *P. aeruginosa* laboratory WT strain PAO1 (60).

Activation of host T2Rs by bacterial quinolones may play a role in innate immune detection of these bacteria. Here, we tested responses of human T2Rs to three bacterial quinolones by live-cell imaging of HEK293T cells heterologously expressing known airway T2Rs and bronchial epithelial cell lines that endogenously express T2Rs. We also tested responses in primary human sinonasal epithelial cells cultured at the air–liquid interface (ALI), a standard model for recapitulating a differentiated airway epithelium *in vitro* (61–63).

Results

PQS and HHQ activate T2R-dependent Ca^{2+} signals in a heterologous expression system

Using the open-access online BitterX program that predicts the "bitterness" of a molecule (64), PQS and DHQ were predicted to activate several T2Rs (Table S1), including T2R4, -14, and -16, which are expressed in sinonasal (9, 12, 14, 31, 32) and bronchial (10) motile cilia. HHQ was determined by this program not to be an activator of T2Rs (Table S1).

We screened PQS, DHQ, and HHQ against HEK293T cells heterologously expressing several human T2Rs plus a G-protein chimera, $G\alpha_{16}$-gust44, that couples the receptors to robust $[Ca^{2+}]_i$ signals. This is a common model system used for determining whether compounds activate specific T2Rs (45, 46) and is frequently used in other GPCR drug discovery assays (65, 66). We focused primarily on the T2Rs expressed in sinonasal cilia (10, 12, 31, 32). Cells transfected with $G\alpha_{16}$-gust44 alone were used as a negative control. PQS (100 μM) activated several T2Rs (Fig. 1 (*b* and *c*) and Fig. S1). Responses were larger when only responsive cells (probably those that were transfected) were selected (Fig. S1), but we chose to determine the statistical significance of the response based on the entire population (Fig. 1) to reduce any potential biasing. The most robust Ca^{2+} responses were with T2R4 and T2R16, but some activation of T2R38 was also observed. HHQ significantly activated only T2R14, whereas DHQ activated no T2Rs examined here (Fig. 1, *d* and *e*). No effects were observed with the highest concentration of vehicle used in these experiments (0.1% DMSO) (Fig. S2) (31).

We tested the dose dependence of PQS against T2R4 (Fig. 2, *a* and *b*) and found a statistically significant elevation of Ca^{2+} as low as 10 μM (10^{-5} M). Whereas $[Ca^{2+}]_i$ responses to PQS were lower than those observed with ATP or quinine (Fig. 2*b*), we did not reach receptor saturation at the maximal concentrations (100–200 μM) that could be achieved in aqueous solution. This is common in studies of T2R agonists (45–47, 67), which are often highly hydrophobic. PQS solubility may be enhanced during infections by *P. aeruginosa* production of rhamnolipid surfactants (68). Nonetheless, these data sup-

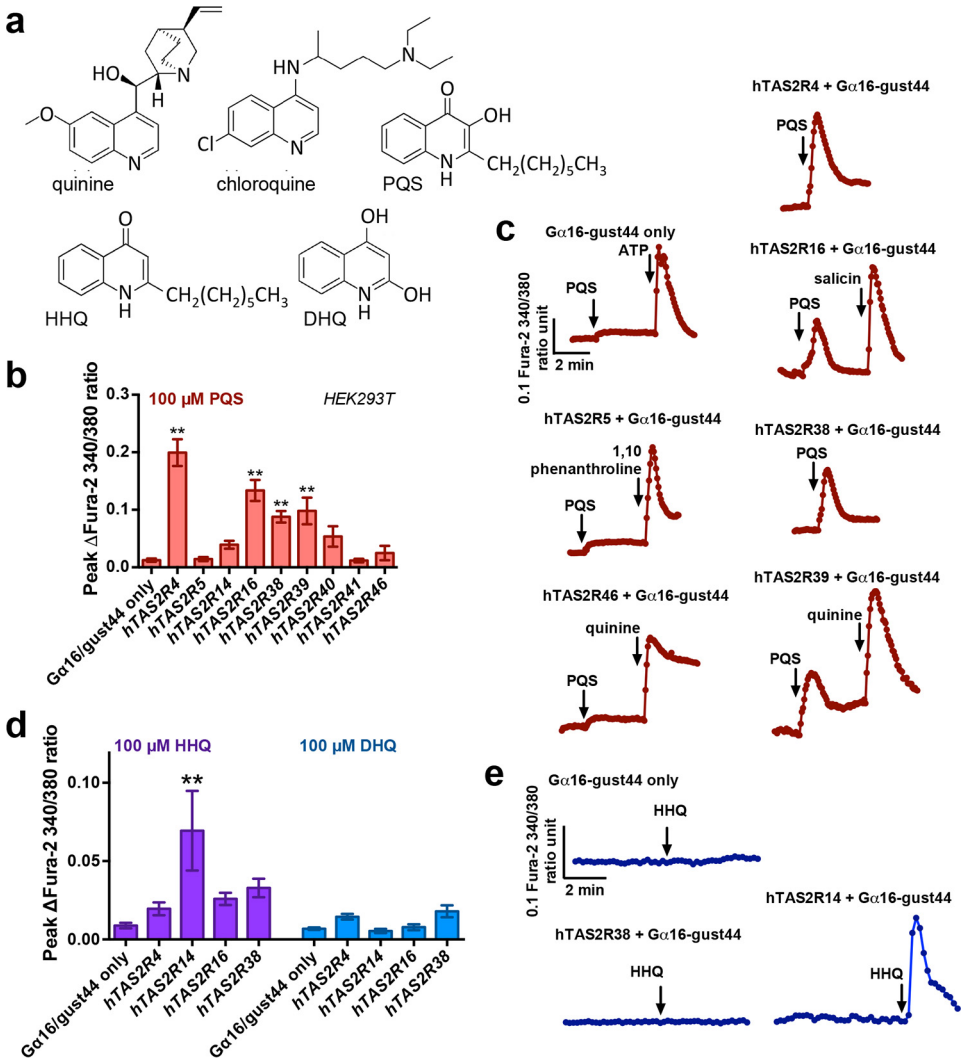

Figure 1. *P. aeruginosa* quinolones activate multiple T2Rs. *a*, chemical structures of quinine ((*R*)-[(2*S*,5*R*)-5-ethenyl-1-azabicyclo[2.2.2]octan-2-yl]-(6-methoxyquinolin-4-yl)methanol), chloroquine (4-*N*-(7-chloroquinolin-4-yl)-1-*N*,1-*N*-diethylpentane-1,4-diamine), PQS (2-heptyl-3-hydroxy-4(1*H*)-quinolone), HHQ (4-hydroxy-2-heptylquinolone), and DHQ (2,4-dihydroxyquinolone). *b*, peak $[Ca^{2+}]_i$ responses of T2Rs to 100 μM PQS in HEK293Ts transfected with $G\alpha_{16}$/gust44 alone or $G\alpha_{16}$/gust44 plus human (*h*) *TAS2R4*, *TAS2R5*, *TAS2R14*, *TAS2R16*, *TAS2R38* (PAV isoform), *TAS2R39*, *TAS2R40*, *TAS2R41*, or *TAS2R46*. *c*, representative trace of PQS response in $G\alpha_{16}$/gust44 only-transfected cells as well as cells transfected with $G\alpha_{16}$/gust44 plus *hTAS2R5* or *hTAS2R46* (which did not respond to PQS) or hTAS2R4, hTAS2R16, hTAS2R38, or hTAS2R39 (which responded to PQS). Results in *b* and *c* were obtained by measuring the entire cell population (entire field of view, containing both transfected and nontransfected cells); peak responses when specific responding cells were selected are shown in Fig. S1 for comparison. Responses were larger when only responding cells were selected, but taking the entire population measurement removes potential biasing. *d*, peak $[Ca^{2+}]_i$ responses (from the entire population as in *b*) with 100 μM DHQ and 100 μM HHQ in HEK293Ts transfected with $G\alpha_{16}$/gust44 alone or $G\alpha_{16}$/gust44 plus *hTAS2R4*, *TAS2R14*, *TAS2R16*, or *TAS2R38*. *e*, representative trace of HHQ response in *hTAS2R14* + $G\alpha_{16}$/gust44–transfected and $G\alpha_{16}$/gust44 only–transfected cells. Bar graphs in *b* and *d* show mean ± S.E. (*error bars*) of 4–10 independent experiments/condition. Significance was determined by one-way ANOVA with Dunnett's post-test using $G\alpha_{16}$/gust44 only–transfected cells as control: *, $p < 0.05$; **, $p < 0.01$.

port detection of PQS by T2R4-transfected cells at concentrations reported to be produced in *P. aeruginosa* cultures (20–30 μM) (48).

To confirm that T2R4 itself is a PQS receptor and that PQS is not sensed by another receptor produced by HEK293T cells in response to T2R4 transfection, we tested the effects of PQS in the presence of GABA, a T2R4 blocker (69). Responses to PQS, but not the purinergic receptor agonist ATP, were diminished in T2R4-expressing cells in the presence of GABA (Fig. 2*c*). We similarly tested the multidrug resistance transporter inhibitor probenecid, an allosteric inhibitor of T2R16 (70). Probenecid pretreatment (1 mM for 1 h, as described (70)) reduced T2R16-dependent $[Ca^{2+}]_i$ responses to both PQS and T2R16-agonist salicin, but not purinergic receptor agonist ATP (Fig. 2*d*). When cells were transfected with the AVI variant of *TAS2R38*, which encodes a nonfunctional T2R38 (22), responses to both PQS and T2R38-agonist phenylthiocarbamide (PTC) were lost (Fig. 2*e*). Responses were only observed with functional PAV *TAS2R38* (Figs. 1 (*b* and *c*) and 2*e*). Together, these results suggest that several T2Rs expressed in the airway can detect bacterial quinolones, including T2R38, which has been implicated in chronic rhinosinusitis (12, 23, 25–29, 71).

PQS and HHQ activate Ca^{2+} signals in lung epithelial cells

We tested PQS against several airway cell lines endogenously expressing T2Rs. The canonical T2R signaling pathway involves Ca^{2+} release downstream of G$\beta\gamma$ activation of phospholipase C (PLC) isoform β2 (PLCβ2; Fig. 3*a*) (9). A549 cells

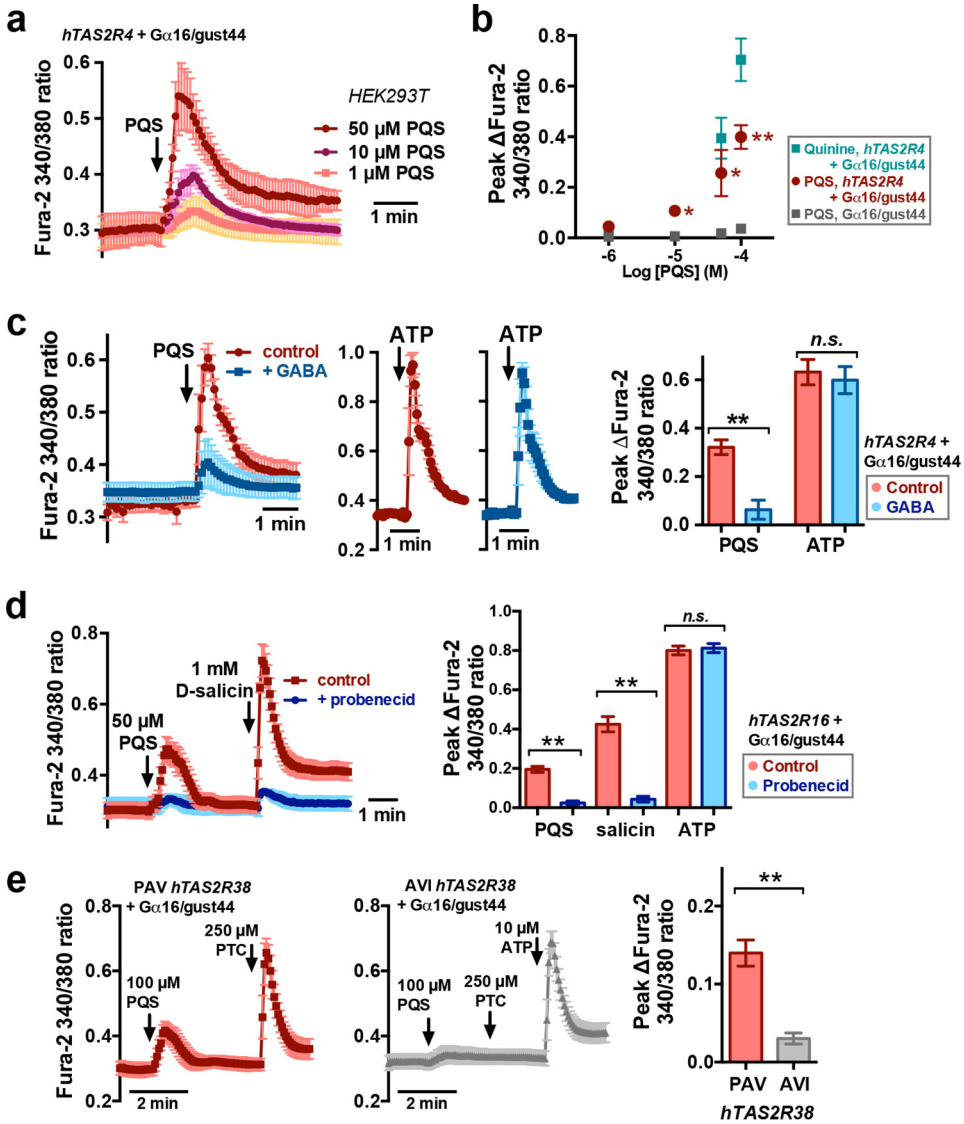

Figure 2. Pharmacology of PQS-activated heterologously expressed T2R Ca^{2+} responses. *a* and *b*, dose dependence of PQS activation of T2R4; $n = 4–6$ independent experiments/condition. The significance of peak $[Ca^{2+}]_i$ values in *b* was determined by one-way ANOVA with Bonferroni (paired comparison) post-test comparing *hTAS2R4* + $G\alpha_{16}$/gust44 *versus* $G\alpha_{16}$/gust44-only cells stimulated with PQS at each concentration. *c*, mean traces and bar graph (*right*) of PQS and ATP responses in HEK293T cells expressing *hTAS2R4* + $G\alpha_{16}$/gust44 in the absence (*red*) or presence (*blue*) of 200 μM GABA. Significance was determined by one-way ANOVA with Bonferroni post-test; $n = 4–6$ independent experiments/condition. *d*, mean traces and bar graph (*right*) of PQS and salicin responses in HEK293T cells transfected with *hTAS2R16* in the absence (*red*) or presence (*blue*) of probenecid. Significance was determined by one-way ANOVA with Bonferroni (paired comparison) post-test; $n = 4–6$ independent experiments for each condition. *e*, mean traces and bar graph of PQS responses in HEK293T cells transfected with PAV (functional; *red*) or AVI (nonfunctional; *gray*) *hTAS2R38* isoforms. Significance was determined by Student's *t* test with $n = 5$ independent experiments/condition: *, $p < 0.05$; **, $p < 0.01$. *Error bars*, S.E.

are an alveolar type 2 adenocarcinoma cell line previously shown to express T2R4 as well as Gα gustducin ($G\alpha_{gust}$; GNAT3) (72). A549 cells exhibited Ca^{2+} responses to both quinine and PQS (Fig. 3*b*). BEAS-2B cells are SV-40–immortalized bronchial cells that also express T2Rs (72) and exhibited Ca^{2+} responses to the T2R10/14 agonist thujone (previously shown to activate T2Rs in primary bronchial cell cilia (10)), but not the T2R38-specific PTC (Fig. 3*c*). BEAS-2B cells also responded to 100 μM PQS (Fig. 3*c*). NCI-H292 (H292) cells are a bronchial mucoepidermoid carcinoma cell line expressing at least one T2R, T2R14 (73). H292 cells also responded to both thujone and PQS (Fig. 3*d*). The PQS response was lost in the presence of the PLC inhibitor U73122 but not its inactive analogue U73343 (Fig. 3*e*). DHQ, which did not activate the airway T2R isoforms tested in HEK293T cells above, did not activate Ca^{2+} responses in BEAS-2B or H292 cells (Fig. 3*f*).

Ca^{2+} elevation in response to PQS stimulation depended on ER Ca^{2+} release, as it was absent in BEAS-2B cells after Ca^{2+} store depletion by either treatment with the SR/ER Ca^{2+} ATPase inhibitor thapsigargin in Ca^{2+}-free (0-Ca^{2+}) extracellular solution (no added Ca^{2+} + 2 mM EGTA) (Fig. S3*a*) or purinergic stimulation with ATP in Ca^{2+}-free extracellular solution (Fig. S3*b*). Pretreatment of BEAS-2B cells with the IP_3 receptor inhibitor xestospongin C (74) likewise blocked the PQS $[Ca^{2+}]_i$ response (Fig. S3*c*). We also treated H292 cells with the G$\beta\gamma$ inhibitor gallein (75) (Fig. S3*d*), which was shown to block bitter agonist signaling in smooth muscle in some studies (76, 77) but not another (78). Gallein significantly reduced

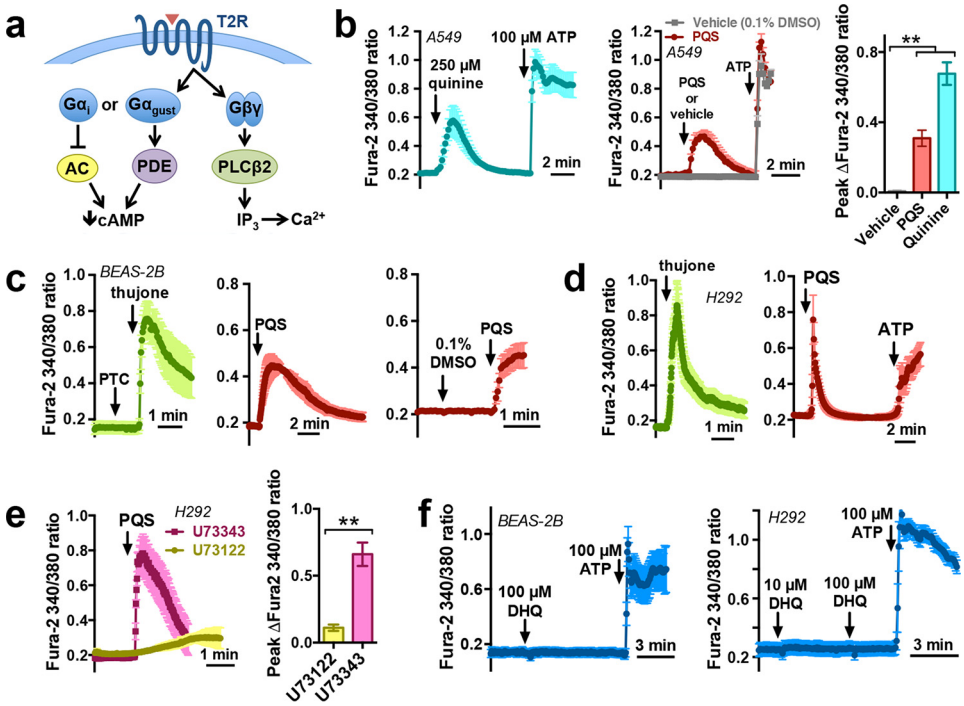

Figure 3. PQS activates Ca^{2+} signals in cultured airway cell lines. *a*, diagram of canonical T2R receptor signaling, which involves Gα-gustducin ($G\alpha_{gust}$) activation of PDE or $G\alpha_i$ inhibition of adenylyl cyclase and lowering of cAMP in addition to $G\beta\gamma$ activation of PLCβ2, which generates IP_3 and activates Ca^{2+} release from the IP_3 receptor ER Ca^{2+} release channel. *b*, mean traces and bar graph of quinine-induced (*cyan*), PQS-induced (100 μM; *red*), or vehicle-induced (0.1% DMSO; *gray*) $[Ca^{2+}]_i$ (n = 3–4 independent experiments/condition). Significance was determined by one-way ANOVA, Dunnett's post-test. *c*, mean $[Ca^{2+}]_i$ in BEAS-2B cells in response to thujone (1 mM; green) or 100 μM PQS (*red*); n = 4–6 independent experiments/condition. *d*, mean $[Ca^{2+}]_i$ responses to thujone or PQS in NCI-H292 (H292) cells; n = 4–6 independent experiments for each condition. *e*, mean traces and bar graph of $[Ca^{2+}]_i$ responses to PQS after pretreatment with PLCβ2 inhibitor U73343 (*yellow*) or inactive U73343 (*pink*; 1 μM each); n = 4 independent experiments/condition. *f*, mean traces showing lack of $[Ca^{2+}]_i$ response to DHQ in BEAS-2B cells (*a*) and H292 cells (*b*); n = 3–5 independent experiments each. Significance was determined by Student's t test (*b* and *e*): **, $p < 0.01$. *Error bars*, S.E.

the $[Ca^{2+}]_i$ elevation with PQS (Fig. S3*d*), supporting a role for $G\beta\gamma$ signaling in this response.

To confirm the Ca^{2+} responses to quinolones observed with small-molecule Ca^{2+} indicators, we transfected BEAS-2B cells with a genetically encoded green Ca^{2+}-sensitive protein, GCaMP6s (79). BEAS-2B cells exhibited an increase in GCaMP6s fluorescence, signaling an increase in Ca^{2+}, in response to PQS, HHQ, and the T2R10/14 agonist thujone (45) (Fig. S4, *a–c*). The PQS Ca^{2+} response observed with GCaMP6s was likewise inhibited by U73122 (Fig. S4*d*), supporting a requirement for receptor-mediated activation of PLC.

Because HHQ appeared to activate only one known airway-expressed T2R isoform, T2R14, we examined the HHQ response in T2R14-expressing (73) H292 cells co-transfected with GCaMP6s (to identify transfected cells and measure Ca^{2+} responses) and two different sets of two shRNA constructs directed against T2R14. HHQ stimulated robust Ca^{2+} responses in H292 cells transfected with GCaMP6s only (Fig. 4*a*) or GCaMP6s + scramble shRNA (Fig. 4*b*). Both sets of distinct T2R14-directed shRNAs markedly reduced the response (Fig. 4, *c* and *d*), whereas the purinergic or protease-activated receptor 2 (PAR-2) GPCR responses were not significantly affected by these shRNA vectors (Fig. 4*e*). These results support a role for endogenous T2R14 in detection of HHQ by lung epithelial cells.

PQS and HHQ decrease baseline and stimulated cAMP levels in lung epithelial cells

The other arm of the canonical T2R signaling pathway (Fig. 3*a*) is $G\alpha_{gust}$, a Gα protein of the transducin family (80–83) which activates phosphodiesterase (PDE). Several airway cell lines have been reported to express $G\alpha_{gust}$ (72, 84), although $G\alpha_i$ isoforms, which inhibit adenylyl cyclases, couple to T2Rs in airway smooth muscle (85). To test whether quinolones activated a $G\alpha_{gust}/G\alpha_i$ pathway, we monitored cAMP dynamics in real time in living cells using a high-affinity fourth-generation Turquoise (CFP)/Venus (YFP) FRET-based EPAC cAMP indicator, EPAC-S^{H187} (86). This construct was previously used to image a decrease in baseline cAMP levels in HEK293T cells expressing $G\alpha_{i/o}$-coupled μ-opioid receptors (87). BEAS-2B cells transfected with EPAC-S^{H187} and stimulated with PQS or quinine exhibited decreases in baseline CFP/FRET emission ratio, signaling decreases in cAMP concentration (Fig. 5*a*). The adenylyl cyclase activator forskolin was used as a control. PQS also blunted cAMP increases during the simultaneous addition of the $G\alpha_s$-coupled β-adrenergic receptor agonist isoproterenol (100 μM; Fig. 5*b*). Similar PQS-induced decreases in baseline cAMP were observed in A549 cells (Fig. 5*c*). When we tested HHQ and DHQ in H292 cells, we observed a decrease in baseline cAMP with HHQ but not DHQ (Fig. 5*e*), as would be expected if HHQ activates T2Rs and DHQ does not. PQS-mediated cAMP decreases were not observed when BEAS-2B cells

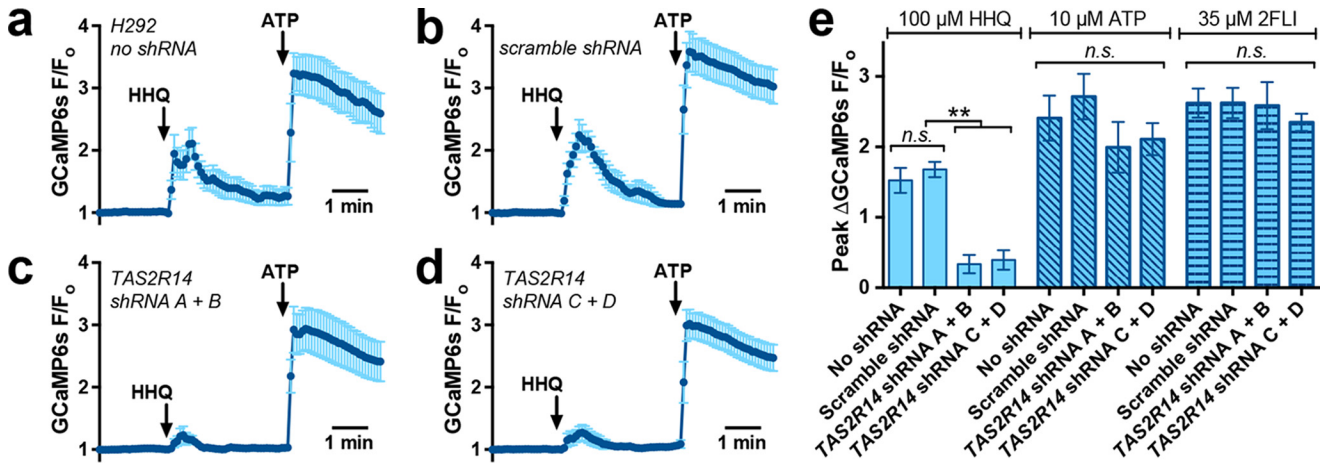

Figure 4. HHQ-activated Ca^{2+} responses are blocked by shRNAs directed against T2R14. *a–d*, mean ± S.E. (*error bars*) traces of GCaMP6s fluorescence (normalized to initial fluorescence; F/F_o) in H292 cells in the absence (*a*) or presence (*b–d*) of co-transfected shRNA plasmids (sequences described under "Materials and methods"). *e*, bar graph of peak GCaMP6s-measured Ca^{2+} responses from individual experiments during stimulation with HHQ (as shown in *a–d*), ATP, or PAR-2 agonist 2FLI (134); n = 7–9 (HHQ) or 3–5 (ATP and 2FLI) independent experiments for each condition; **, $p < 0.01$; *n.s.*, no statistical significance.

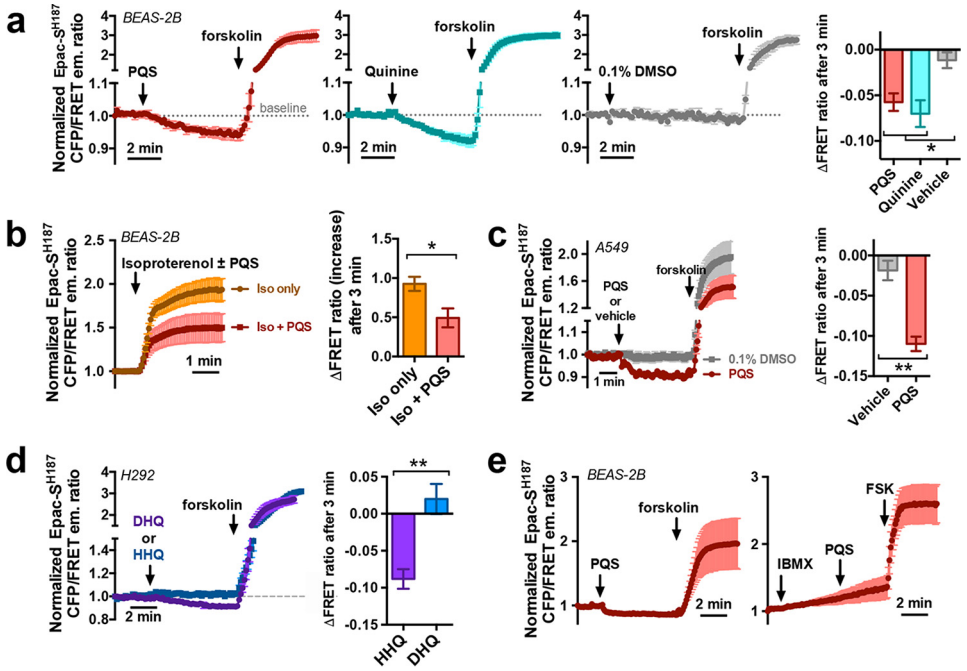

Figure 5. PQS and HHQ, but not DHQ, attenuate baseline and stimulated cAMP levels in airway epithelial cell lines. *a*, mean traces and bar graph of normalized (baseline = 1) EPAC-S^{H187} CFP (430/24-nm band pass excitation, 470/24-nm emission) over FRET (430/24-nm excitation; 535/30-nm emission) ratio in transfected BEAS-2B cells stimulated with quinine (100 μM, dissolved directly in HBSS; *cyan*), PQS (100 μM; *red*), or PQS vehicle (0.1% DMSO; *gray*). A *downward deflection* reflects a decrease in cAMP, and vice versa; n = 3–4 independent experiments/condition; each experiment simultaneously imaged at least three transfected cells. Forskolin (10 μM) was a positive control to increase cAMP. *b*, mean trace and bar graph of EPAC-S^{H187} CFP/FRET ratio in BEAS-2B cells stimulated with isoproterenol (100 μM) with or without PQS (100 μM); n = 4 independent experiments for each condition. *c*, mean trace and bar graph of EPAC-S^{H187} CFP/FRET ratio in A549 cells with or without PQS; n = 5–6 independent experiments for each condition. *d*, trace of EPAC-S^{H187} fluorescence emission in H292 cells stimulated with HHQ (*blue*) or DHQ (*purple*); n = 4–6 independent experiments/condition. All traces and bar graphs show mean ± S.E. (*error bars*). *e*, trace of PQS-induced EPAC-S^{H187} fluorescence changes in the absence (*left*) or presence (*right*) of phosphodiesterase inhibitor IBMX (100 μM); n = 3–5 independent experiments. Significance by one-way ANOVA with Bonferroni post-test (*a*) or Student's *t* test (*b–d*): *, $p < 0.05$; **, $p < 0.01$.

were treated with IBMX, a phosphodiesterase inhibitor (Fig. 5*f*), suggesting $G\alpha_{gust}$ activation of phosphodiesterase. A similar result was observed in H292 cells (Fig. S5).

To confirm that this change in EPAC construct fluorescence was due to activity of a $G\alpha_{gust}/G\alpha_o/G\alpha_i$ protein, we treated BEAS-2B cells with pertussis toxin (PTX; 500 ng/ml; 18 h), which ADP-ribosylates and inactivates $G\alpha_{gust}$, $G\alpha_o$, and $G\alpha_i$ subunits (76, 88, 89). PTX reduced the cAMP decrease observed with PQS and HHQ (Fig. 6, *a* and *b*), suggesting a role for a $G\alpha_{gust}/G\alpha_o/G\alpha_i$-linked receptor. We co-transfected BEAS-2B cells with EPAC-S^{H187} and the $G\alpha_{16}$/gust44 chimera used in HEK293T cells above. $G\alpha_{16}$ is a $G\alpha_q$, which activates PLC instead of PDE, and the C-terminal $G\alpha_{gust}$ portion will bind to T2Rs (45, 65–67). We hypothesized that overexpression of $G\alpha_{16}$/gust44 would out-compete endogenous $G\alpha_{gust}$ or $G\alpha_i$ proteins and reduce cAMP decreases. BEAS-2B cells co-transfected with WT $G\alpha_{gust}$ and EPAC-S^{H187} exhibited PQS-stimulated cAMP decreases similar to cells transfected with

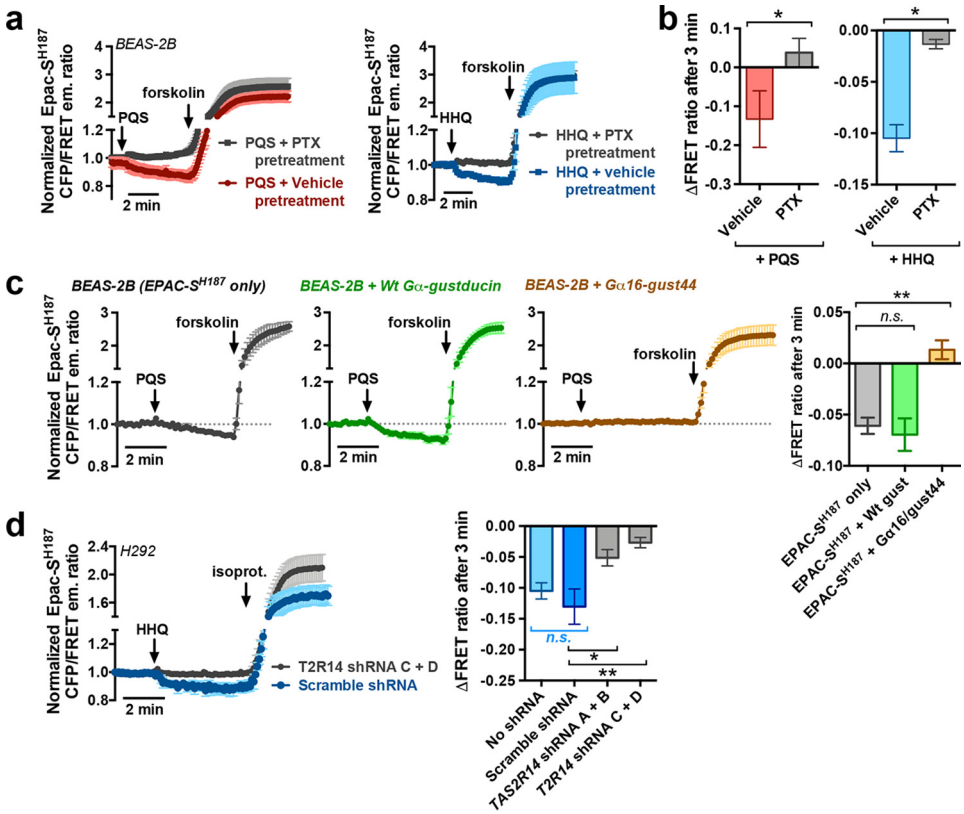

Figure 6. PQS- and HHQ-induced cAMP decreases were mediated by a $G\alpha_{i/o/gust}$ pathway that probably involves T2Rs. *a* and *b*, mean traces (*a*) and bar graph (*b*) of CFP/FRET emission ratio in EPAC-S^{H187}-transfected BEAS-2B cells pretreated with PTX followed by stimulation with PQS or HHQ; $n = 3–6$ independent experiments/condition. *c*, mean traces and bar graph of normalized change in EPAC-S^{H187} FRET ratio in BEAS-2B cells co-transfected with WT gustducin (*green*) or $G\alpha_{16}$/gust44 (*orange*); $n = 4–7$ independent experiments/condition. *d*, mean traces and bar graph of H292 cells co-transfected with EPAC-S^{H187} and either scramble or T2R14-directed shRNA plasmids; $n = 4–6$ experiments/condition. *, $p < 0.05$; **, $p < 0.01$; significance was determined by Student's *t* test (*b*) or one-way ANOVA with Dunnett's post-test (*c* and *d*). *Error bars*, S.E.

EPAC-S^{H187} only (Fig. 6*c*). However, $G\alpha_{16}$/gust44-expressing cells did not exhibit cAMP decreases (Fig. 6*c*) but still exhibited cAMP increases with forskolin, demonstrating that EPAC-S^{H187} remained functional. When H292 cells were co-transfected with shRNAs to T2R14 and EPAC-S^{H187}, the baseline cAMP decrease observed with HHQ was undetectable (Fig. 6*d*).

To confirm the effects of quinolones on cAMP, we utilized another cAMP indicator, Flamindo2 (90). BEAS-2B cells transfected with Flamindo2 exhibited a PQS dose-dependent inhibition of isoproterenol-induced cAMP increases, evidenced by a decrease in Flamindo2 fluorescence (Fig. S6). The cAMP increase activated by 100 nM isoproterenol was inhibited dose-dependently by PQS (1–100 μM; Fig. S6, *a* and *b*), with the rate of Flamindo2 fluorescence change inhibited ~10-fold by 100 μM PQS (Fig. S6*c*). Moreover, in H292 cells transfected with Flamindo2, HHQ (100 μM) inhibited cAMP increases in response to 100 nM isoproterenol (Fig. S7). The effect of HHQ was substantially reduced when cells were co-transfected with shRNAs directed against T2R14 but not scrambled shRNA (Fig. S7).

The data above suggest that PQS and HHQ activate Ca^{2+} through $G\beta\gamma$ activation of PLC and decrease cAMP through a PTX-sensitive $G\alpha$, as would be expected during T2R stimulation and activation of $G\alpha_{gust}$. To test whether this change in baseline cAMP affects baseline protein kinase A (PKA) activity, we transfected BEAS-2B cells with a PKA-sensitive CFP/YFP construct, AKAR4 (91). BEAS-2B cells exhibit baseline PKA activity even in the absence of any stimulation, evidenced by the ability of the PKA inhibitor H89 to reduce AKAR4 FRET/CFP emission ratio (Fig. 7*a*), signifying a decrease in PKA activity. Even when cells were stimulated with forskolin to increase PKA activity, H89 was able to bring PKA activity back to a level below the initial baseline (Fig. 7*a*). PQS also caused a drop in baseline PKA activity (Fig. 7*b*). As a control, we expressed the protein kinase C–sensitive CFP/YFP construct CKAR (92) in BEAS-2B cells and observed no change in CKAR fluorescence despite a change with the diacylglycerol mimetic phorbol 12-myristate 13-acetate (PMA) (Fig. 7*c*). This suggests that PQS does not stimulate protein kinase C activation (not previously reported for taste receptors) but also that quinolones do not have non-specific effects on the CFP or YFP variants in these fluorescent constructs.

Bacterial quinolones activate Ca^{2+} signals and decrease cAMP levels in primary sinonasal epithelial ALI cultures

We isolated primary sinonasal epithelial cells from residual surgical material and cultured them at the ALI, which causes differentiation into ciliated and goblet cells and mimics the *in vivo* airway epithelium (61). The ciliated cells in sinonasal and bronchial ALIs express T2R4, -14, -16, and -38 similarly to tissue explants (10, 12, 31, 32). We previously showed that T2R14 and -38 are co-localized closely enough to observe FRET when

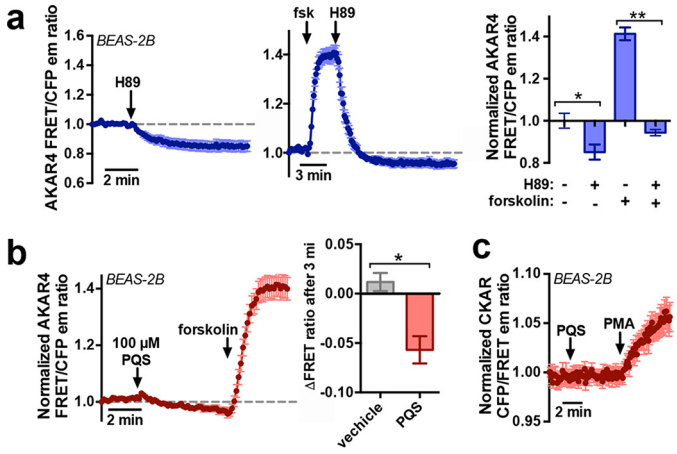

Figure 7. PQS reduces baseline PKA signaling in BEAS-2B bronchial epithelial cells. *a*, mean trace of H89 (10 μM)-induced AKAR4 fluorescence emission changes in the absence of prior stimulation (*left*) or after stimulation with forskolin (10 μM; *middle*). A *downward deflection* reflects a decrease in PKA activity, whereas an *upward deflection* reflects an increase in PKA activity. The bar graph (*right*) shows normalized AKAR4 emission ratio after 3 min; $n = 5–8$ independent experiments. Significance was determined by one-way ANOVA with Bonferroni post-test (paired comparisons). *b*, AKAR fluorescence changes in response to PQS (mean trace, *left*). Bar graph (*right*) shows change in AKAR fluorescence after 3 min in response to PQS (100 μM) or vehicle (0.1% DMSO); $n = 4–6$ independent experiments for each condition. Significance was determined by Student's *t* test. *c*, mean trace of CKAR fluorescence in BEAS-2B cells stimulated with PQS (100 μM) or PMA (100 nM); $n = 5$ independent experiments. *, $p < 0.05$; **, $p < 0.01$. *Error bars*, S.E.

primary antibodies were labeled with Alexa Fluor (AF)-conjugated Fab fragments (31). In contrast, T2R4 is localized to only the distal tips of motile cilia (10, 31) (Fig. 8, *a* and *b*).

We examined the colocalization of cilia T2R16 and T2R38 (Fig. S8*a*) using the same method used previously for T2R38 and T2R14 (31) with antibodies directed against the C terminus of both proteins. FRET was observed between T2R16 and T2R38 when both primary antibodies were labeled with either a donor (AF555) or acceptor (AF647) fluorophore (Fig. S8*b*). Acceptor bleaching increased donor fluorescence (Fig. S8*c*) 20 ± 1% when T2R38 was used as the donor and T2R16 as the acceptor and 22 ± 1% with donor T2R16 and acceptor T2R38-directed antibodies (*n.s.*; Fig. S8*d*). Donor fluorescence increase with acceptor bleaching is roughly equivalent to FRET efficiency. When the two groups pooled, mean FRET efficiency was 21 ± 1%, similar to the efficiency (16 ± 2%) observed previously with T2R38 and T2R14 (31). The Förster radius (R_o) is the distance at which FRET efficiency is 50%, which is 51 Å for this FRET pair. Efficiency (E) decreases to the 6th power as distance (R) increases. Thus, $R = R_o \cdot ((1 - E)/E)^{1/6}$. With $E = 0.21$, $R = 51$ Å$\cdot((1 - 0.21)/0.21)^{1/6} = 64$ Å. Thus, when bound to the C terminus of T2R38 and T2R16, our labeled antibodies are on average 6.4 nm apart. We cannot conclude from these or prior (31) data that T2R38, -16, or -14 forms heterodimers due to the sizes of the antibodies involved, but similar antibody-based measurements have been used to suggest a "close association" of endogenously expressed proteins (93).

Stimulation of T2Rs in sinonasal cilia activates small but sustained Ca^{2+} responses (12, 14, 31). We observed similar Ca^{2+} responses during PQS stimulation of sinonasal ALIs (Fig. 8, *c* and *d*). As with T2R38, the sustained phase of the Ca^{2+} response required Ca^{2+} influx, as the signal decayed over the course of 3–4 min in the absence of extracellular Ca^{2+} (0-Ca^{2+} solution containing 2 mM EGTA) (Fig. 8*e*). Once differentiated, ALIs are difficult to transfect even with viral vectors, and thus we could not use EPAC-S^{H187} or AKAR4 in primary cells. However, we measured cAMP during forskolin and isoproterenol stimulation using a high-sensitivity cAMP ELISA and found that co-stimulation with PQS (10–100 μM) decreased stimulated cAMP (Fig. 9*a*), and this effect was blocked by PTX pretreatment (Fig. 9*b*), fitting with PQS activation of a $G\alpha_{gust}$ or $G\alpha_i$. Because baseline cAMP levels were below the limit of detection of this ELISA, we could not quantify baseline cAMP changes using this method.

P. aeruginosa quinolones activate NO production in primary sinonasal ALI cultures

A hallmark of T2R stimulation in primary differentiated sinonasal ciliated cells is activation of Ca^{2+}-dependent NOS (probably endothelial NOS) (12, 14, 31, 32, 87). NO can damage bacterial cell walls and DNA (19, 20). We showed that airway T2R38-mediated NO production is bactericidal against *P. aeruginosa* (12, 14, 18). Apical application of PQS activated an increase in fluorescence of ALIs loaded with the fluorescent indicator DAF-FM (Fig. 10, *a* and *b*), which exhibits an increase in fluorescence quantum yield when it reacts with reactive nitrogen species (RNS) like NO and its reactive derivatives. There was an additive effect when PQS was combined with HHQ and DHQ (Fig. 10, *a* and *b*), and similar DAF-FM fluorescence increases were observed with quinine (Fig. 10, *a* and *b*). RNS typically react to generate NO_2^- or NO_3^- products. We used a fluorometric assay based on the Greiss reaction to measure total $NO_2^- + NO_3^-$ in fluid overlaying the apical surface of sinonasal ALIs stimulated for 18 h with the T2R4/14 agonist quinine, T2R38 agonist PTC, T2R14 agonist flufenamic acid (FFA), or PQS. Cultures were also genotyped for *TAS2R38* PAV (functional) *versus* AVI (nonfunctional) polymorphism status. NO_2^-/NO_3^- levels were increased in cultures homozygous for the PAV haplotype (PAV/PAV) stimulated with all T2R agonists (Fig. 10*c*). AVI/AVI cultures also exhibited NO increases to all agonists except PTC (Fig. 10*c*). Whereas the PQS response appeared to be slightly lower, it was not statistically significantly different from PAV/PAV cultures (Fig. 10*c*). However, when AVI/AVI cultures were stimulated with PQS in the presence of GABA (to block T2R4) and probenecid (to block T2R16), NO production was significantly reduced (Fig. 10*d*). In the presence of GABA and PQS, we noted a significant difference between NO production between PAV/PAV and AVI/AVI cultures (Fig. 10*e*). Thus, under conditions of T2R4 and T2R16 blockade, the response is altered by T2R38 functionality, strongly suggesting a role for T2R receptors in this response.

Discussion

The data here support the hypothesis that T2Rs can detect bacterial quinolones and that this may play a role in innate immune signaling in airway epithelia. This supports a role for T2Rs in mediating interkingdom signaling through mammalian cell detection of bacterial metabolites. We used heterologous expression and multiple airway cell lines to quantitatively image PQS and HHQ responses using fluorescent ion indica-

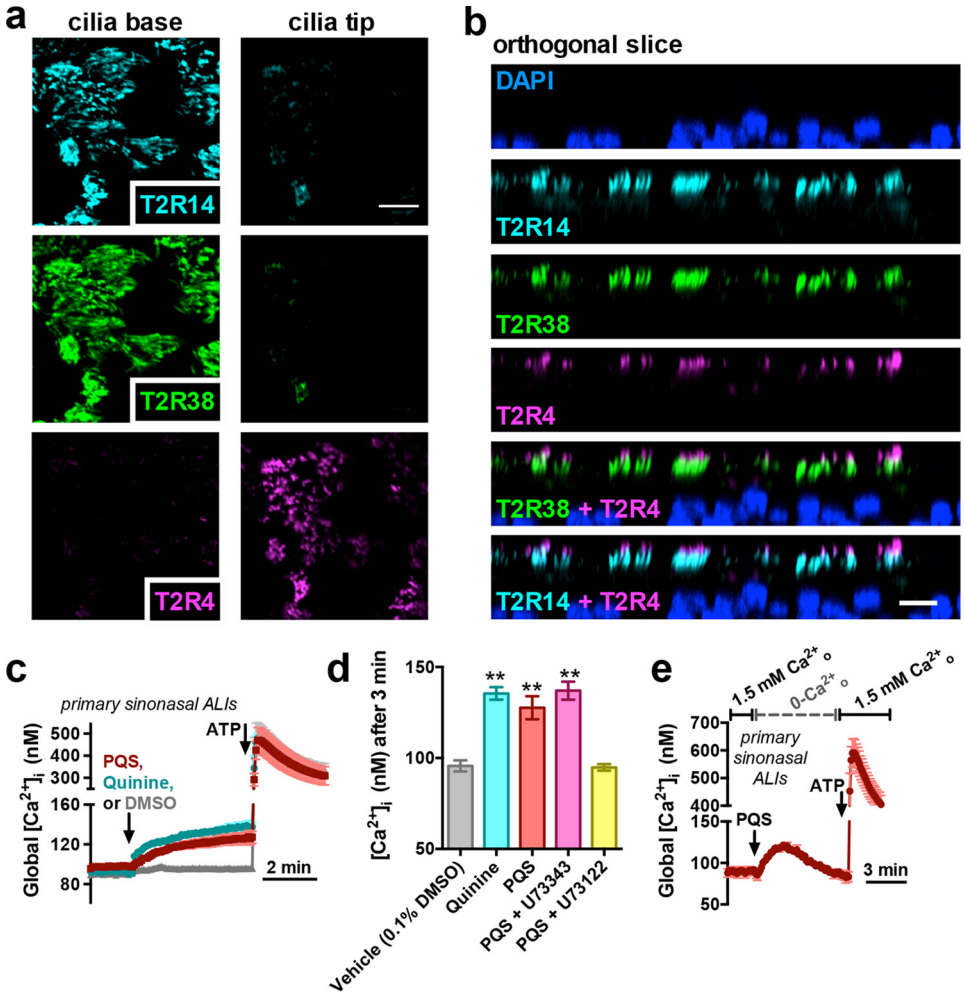

Figure 8. PQS increases Ca^{2+} in primary sinonasal ALIs. *a*, immunofluorescence localization of endogenous T2R4 (*magenta*), T2R14 (*cyan*), and T2R38 (*green*) in primary sinonasal ALI cilia; shown are single confocal slices (*x-y*) in a view looking down on the cilia. Cilia base and tip slices are separated by ~4 μm. *Scale bar*, 10 μm. *b*, orthogonal slice (*x-z*) showing cross-section (no interpolation) of primary sinonasal ALI cilia from an experiment as in *a*. *Scale bar*, 10 μm across the *horizontal direction* only. The vertical (*z*) axis was not calibrated for any refractive index mismatch. *c*, average traces of primary sinonasal ALIs loaded with fura-2 (calibrated to $[Ca^{2+}]_i$) and stimulated with PQS (100 μM; *red*), quinine (100 μM; *cyan*), or DMSO (0.1%; *gray*). *d*, bar graph of mean ± S.E. (*error bars*) $[Ca^{2+}]_i$ 3 min after stimulation with the indicated compounds. U73122 and U73343 were used at 20 μM (20-min pretreatment); $n = 3$–5 experiments for each condition, each experiment with an ALI from a different individual patient. Significance was determined by one-way ANOVA with Dunnett's post-test comparing all conditions with vehicle control. *e*, mean ± S.E. trace of PQS $[Ca^{2+}]_i$ responses in extracellular Ca^{2+}-free conditions (0-Ca^{2+} + 2 mM EGTA); $n = 3$ individual experiments, each using an ALIs from a different individual patient: **, $p < 0.01$. ALIs used in these experiments were from patients genotyped for *TAS2R38* and determined to be PAV/AVI heterozygotes.

tors and FRET-based protein biosensors in real time in living cells. This was combined with quantification of responses in primary cells to validate that the effects observed were not artifacts of one or more cell lines.

In contrast to the BitterX (64) prediction of HHQ as "not bitter," both PQS and HHQ activated different cilia-localized T2Rs, cautioning that experimental testing is always needed to confirm/refute results of computer predictions or modeling. Testing of PQS, HHQ, and DHQ against all 25 T2Rs in future higher-throughput studies will determine the receptors most sensitive for these compounds. We focused on known airway cilia T2Rs to test whether PQS and HHQ detection by T2Rs may be important for epithelial immune surveillance.

Quinine taste sensitivity varies with polymorphisms in a bitter receptor cluster on chromosome 12 (94); T2R14 is located on chromosome 12, whereas T2R4, -16, and -38 are located on chromosome 7. It remains to be determined whether these chromosome 12 polymorphisms affect sensitivities to HHQ or PQS. However, a clinical study recently reported that chronic rhinosinusitis patients with nasal polyps rated quinine as less bitter than control subjects in taste tests, suggesting that a reduced functionality of quinine-responsive T2Rs may play a role in susceptibility to chronic rhinosinusitis (95). Although further clinical investigation is needed, the results presented here suggest that a reduced response to bacterial quinolones may be a mechanism contributing to impaired immunity in patients less sensitive to quinine (95). Taste testing may someday have clinical diagnostic utility in chronic rhinosinusitis or other types of infectious diseases (96).

It is not surprising that bacterial quinolones activate both T2R14 and T2R4, as both are activated by quinine *in vitro*. T2R14 is a receptor with a broad range of activating compounds (97). Whereas it was somewhat surprising that PQS activates T2R4 but not T2R14 and HHQ activates T2R14 but not T2R4, the quinolone chloroquine activates T214 but not T2R4. Thus, there is precedent for differential quinolone recognition

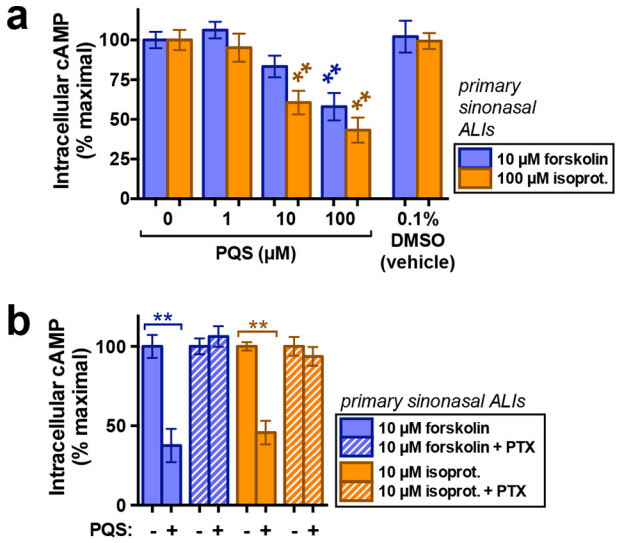

Figure 9. PQS decreases stimulated cAMP levels in primary sinonasal ALIs. *a*, bar graph of cAMP levels in forskolin-stimulated (*purple*) or isoproterenol (*isoprot.*)-stimulated (*orange*) ALIs measured via ELISA and normalized to forskolin or isoproterenol only (maximum stimulation for each condition); $n = 6–10$ ALIs for each condition. All primary ALIs used in experiments in this figure were from patients genotyped for *TAS2R38* and determined to be PAV/AVI heterozygotes. Significance was determined by one-way ANOVA with Dunnett's post-test comparing each group (isoproterenol or forskolin) with the respective control (0-PQS). *b*, bar graph of normalized cAMP production as in *a* but from a separate set of cultures in the absence (*solid bars*) or presence of PTX (*crossed bars*) pretreatment (500 ng/ml; 18 h). Significance was determined by one-way ANOVA with Bonferonni post-test with paired comparisons (0 *versus* 100 μM PQS for each condition); $n = 6–10$ ALI cultures/condition from at least three different patients: **, $p < 0.01$. *Error bars*, S.E.

between the two isoforms. It is most surprising that PQS activated T2R38 and T2R16, albeit to a lesser extent than T2R4. T2R38 and T2R16 are considered to be T2Rs with relatively specific types of activating molecules. T2R38 typically recognizes thiolactones (98), and T2R16 typically recognizes β-glycosides (99). However, exceptions to this specificity have been described. For example, T2R38 is also activated by the alkaloid yohimbine, and T2R16 is activated by the antimuscarinic diphenidol (45), so activation of these two receptors by structurally diverse compounds is not without precedent. Because of the wide range of cilia-localized T2Rs that can be stimulated with quinolone compounds (*e.g.* PQS), quinolones might be useful therapeutics to target this pathway in patients.

Importantly, quinolone T2R responses are not due to DMSO vehicle. A recent publication (100) erroneously reported that our previous studies of AHLs (12, 14) used 3% DMSO. This study found that T2R38 expressed in HEK293T cells is a receptor for many small organic bacterial molecules at high concentrations (>1%), and concluded that prior AHL results were an artifact of 3% DMSO activation of T2R38 (100). However, in all studies, we have consistently utilized 1000× DMSO stock solutions (100 mM) of AHLs and now quinolones, making final DMSO concentrations 0.1% or up to 0.2% if two DMSO-dissolved compounds are added together. We have repeatedly found no effects of these DMSO levels on airway cell Ca^{2+} or NO signaling (12, 14, 15, 31, 101, 102), including here. Moreover, other studies have supported a specific role for T2R38 in AHL detection (103–106) and also found no activation of endogenous T2R38 by 0.1% DMSO (107), as used here.

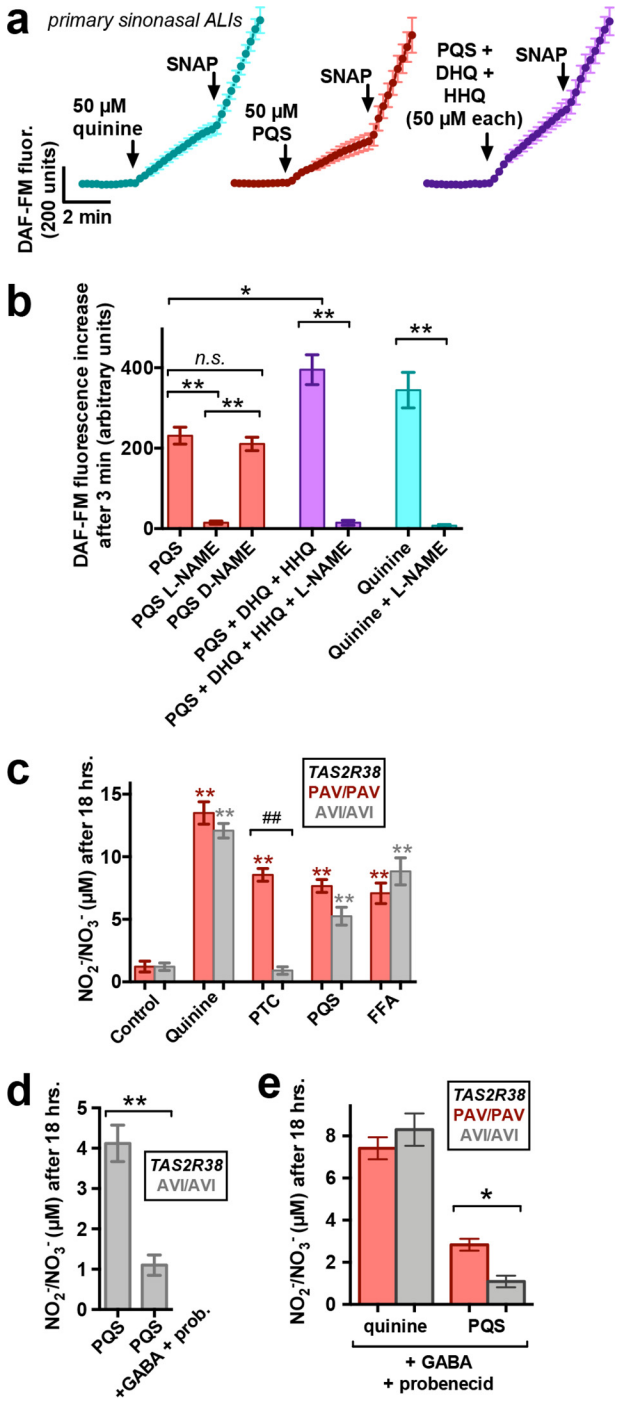

Figure 10. PQS increases NO production from primary sinonasal ALIs. *a*, mean ± S.E. (*error bars*) traces of DAF-FM fluorescence increases in primary sinonasal ALIs stimulated apically with PQS, PQS + DHQ + HHQ, or quinine as indicated. *b*, bar graph of DAF-FM fluorescence increases from experiments as in *a*; $n = 5–7$ experiments for each condition. Significance determined by one-way ANOVA with Bonferroni post-test. *c*, bar graph of NO_2^-/NO_3^- levels in apical fluid collected from primary PAV/PAV or AVI/AVI genotyped sinonasal ALIs stimulated with HBSS only (control), quinine (100 μM), PTC (500 μM), PQS (100 μM), or FFA (100 μM). *Asterisks* represent significance compared with control (unstimulated) conditions), and *number signs* represent significance between the *bracketed groups*. Significance was determined by one-way ANOVA with Bonferroni post-test. *d* and *e*, bar graphs of PAV/PAV and AVI/AVI cultures stimulated with PQS in the presence or absence of GABA and probenecid (pretreatment as above) from separate sets of experiments; $n = 6–10$ ALIs/condition. Significance was determined by Student's *t* test. *, $p < 0.05$; **, $p < 0.01$; ##, $p < 0.01$.

We demonstrate for the first time, to our knowledge, that endogenous T2R activation can have direct effects on baseline cAMP levels and baseline PKA activity in intact airway epithelial cells. It was previously shown that the bitter compound denatonium lowers forskolin-induced cAMP levels in bronchial cells (84). Using state-of-the-art, high-dynamic range, high-affinity FRET indicators (86, 90), we show here that T2R activation by PQS lowers basal unstimulated cAMP levels in addition to stimulated cAMP levels. This may have implications for ion transport in the airway, as the apical cystic fibrosis transmembrane conductance regulator (CFTR) chloride channel is activated by PKA phosphorylation in response to cAMP (108). Future work is needed to understand how T2R activation may affect CFTR function at baseline or during concomitant stimulation of cAMP-elevating pathways.

In addition to *P. aeruginosa*, *Burkholderia* species also produce and respond to quinolones (109). Coupled with previous data showing that T2Rs respond to AHLs (12, 46, 103, 104), the data here support a role for T2Rs similar to other established immune pattern recognition receptors (PRRs), which recognize conserved pathogen-associated molecular patterns that signal the presence of infection. We hypothesize that at least some T2Rs exist in myriad extraoral tissues to detect bacterial and possibly fungal metabolites and activate defensive responses, making them a novel type of immune PRRs.

It is potentially important that both of the known bacterial products that activate airway cilia T2Rs (AHLs, PQS, and HHQ) are metabolites of Gram-negative bacteria. A recent study found that *P. aeruginosa* are more sensitive to the bactericidal effects of NO than Gram-positive *Staphylococcus* or the fungus *C. albicans* (18). Airway ciliated cells are probably the highest sites of NOS activity in the airway epithelium (110–116), and thus ciliated cells may have evolved to express T2Rs that detect Gram-negative metabolites so as to activate this specific defensive pathway in response to the bacteria that are most sensitive to its effects.

PQS induces secretion of IL-8 and IL-6 in human mesenchymal stem cells (117) and stimulates chemotaxis of polymorphonuclear neutrophils (118). Longer-term (4–24-h) stimulation with PQS was recently shown to induce oxidative stress and reduce heme oxygenase-1 expression in A549 cells and J774A.1 and THP-1 macrophage-like cell lines (55). These mechanisms may involve T2Rs. Neutrophils express T2R38 (103, 104) that would probably detect PQS. However, it will be difficult to tease out the relative importance of the PQS and AHL to infection and immune sensing *in vivo*, as the PQS and AHL pathways are intimately intertwined (119, 120). At least one of the genes required for PQS synthesis is controlled by the *N*-3-oxo-dodecanoyl-L-homserine lactone–activated LasR pathway in *P. aeruginosa* (121). Studies have also reported differential positive regulation of PQS by the LasR and negative regulation of PQS by the *N*-butyryl-L-homoserine lactone–activated RhlR pathways (35, 122).

Further work is needed to define other bacterial and/or fungal compounds that activate T2Rs. We previously showed that functional T2R38 is necessary for airway cell NO responses to AHLs. A recent study reported that T2R10 and T2R14, not T2R38, respond to some AHLs when expressed in HEK293 cells (46). The reason for this discrepancy is not yet clear, as other studies have shown that T2R38 detects AHLs (103–106). We hypothesize that cloned receptor polymorphisms and/or different methodologies (microscopy *versus* plate reader assays) may contribute to some differential results observed. Discrepancies in agonist activation extend beyond AHLs (*e.g.* epigallocatechin gallate for T2R14 and genistein for T2R39 (46)). Receptor interactions and/or dimerization may also occur *in vivo* and alter sensitivities. GPCR dimerization frequently has important functional consequences (123, 124). Whereas studies of T2R–T2R interactions so far suggest minimal effect of T2R–T2R dimerization partners (125, 126), these studies have been carried out in heterologous overexpression systems utilizing receptors with tags to help them traffic to the plasma membrane. We believe that, although heterologous expression studies are tremendously useful, such results must be combined with studies of endogenous receptors to better understand T2R signaling *in vivo*. An important example is the recent work demonstrating that T2R14 can heterodimerize with β-adrenergic receptors, important for trafficking to the plasma membrane in airway smooth muscle (73). Continued studies of endogenous T2R signaling are needed to shed light on the cell biology of these receptors and their role in innate immunity and other processes.

Materials and methods

Reagents and solutions

Unless indicated, all reagents and solutions used were as described previously (12, 14, 15, 101, 127). Unless indicated below, all other reagents were from Sigma-Aldrich. Fura-2-acetoxymethyl ester (AM), fluo-4-AM, and DAF-FM diacetate were from Thermo Fisher Scientific (Waltham, MA). Anti-β-tubulin IV (ab11315; mouse monoclonal), anti-T2R38 (ab130503; rabbit polyclonal), anti-T2R16 (ab75106; rabbit polyclonal), xestospongin C, thapsigargin, and 2-furoyl-LIGRLO-amide (2FLI) were from Abcam (Cambridge, MA). Anti-T2R4 (T13, sc169494; goat polyclonal) was from Santa Cruz Biotechnology, Inc. (Dallas, TX). Stock solutions of PQS, HHQ, and DHQ were made at 100 mM in DMSO ($\geq$1000×). PQS has poor aqueous solubility that may be enhanced *in vivo* by bacterially produced biosurfactant rhamnolipids (68). We noted a precipitation and loss of activity of PQS and HHQ after ~30 min in aqueous solution, so working solutions were diluted immediately before use for each experiment with vigorous vortexing (>90 s) before the addition of a 2× working solution (200 μM PQS or HHQ for most experiments) of the compound into a well of a chambered coverglass (CellVis, Mountain View, CA) containing cells and an equal volume of Hanks' balanced salt solution (HBSS).

Sequences of human *TAS2R4*, *TAS2R5*, *TAS2R14*, *TAS2R16*, PAV *TAS2R38* (functional isoform), AVI *TAS2R38* (nonfunctional isoform), *TAS2R39*, *TAS2R40*, *TAS2R41*, and *TAS2R46* were cloned into pcDNA3.1 vectors containing the first 45 amino acids of the rat type 3 somatostatin receptor at the N terminus and an HSV tag at the C terminus to enhance membrane expression, as described previously (126, 128).

EPAC-S^{H187} (mTurq2Δ_Epac(CD,ΔDEP, Q270E)_td^{cp173}Ven) was a kind gift of K. Jalink and J. Klarenbeek (Netherlands Cancer Institute, Amsterdam, The Netherlands). WT gustducin vector was purchased from Cyagen Biosciences (Santa Clara, CA) and confirmed by DNA sequencing (University of Pennsylvania School of Medicine sequencing core). AKAR-4 (91) was from Jin Zhang (Addgene plasmid 61619), GCaMP6s (79) was from Douglas Kim (Addgene plasmid 40753), Flamindo2 (90) was from Tetsuya Kitaguchi (Addgene plasmid 73938), and CKAR (92) was from Alexandra Newton (Addgene plasmid 14860).

Sequences for T2R14 shRNA constructs were expressed via a pRS shRNA expression vector with U6 promoter (HuSH-29; Origene Technologies, Rockville, MD). Sequences for shRNAs were 5′-TTTGGTGCTGCTTCTTGTGACTTCGGTCT-3′ (shRNA A; Origene catalog no. TR301238A), 5′-TCACTGCTTTGGCAATCTCTCGAATTAGC-3′ (shRNA B; catalog no. TR301238B), 5′-CATCGCAAGAAGATGCAGCACACTGTCAA-3′ (shRNA C; catalog no. TR301238C), and 5′-TCTCTGTCAGTGCTACTGTGGCTGAGGTA-3′ (shRNA D; catalog no. TR301238D). Scramble shRNA sequence (catalog no. TR30012) was 5′-GCACTACCAGAGCTAACTCAGATAGTACT-3′.

HEK293T cell culture and transfection

HEK293T cells (ATCC) were cultured in high-glucose DMEM (Gibco) plus 10% FBS. 24 h before transfection, cells were plated on glass coverslips coated with poly-D-lysine. Transfection was carried out with Lipofectamine 2000 according to the manufacturer's instructions. Each T2R was co-transfected with pcDNA3.1 containing $G\alpha_{16}$-gust44, a chimeric $G\alpha$ protein containing $G\alpha_{16}$ (a $G\alpha_q$) fused to the last 44 amino acids of gustducin, as described previously (65, 66, 128). Cells were used 24–48 h after transfection.

Culture of human bronchial cell lines

A549, BEAS-2B, and NCI-H292 cells were obtained from ATCC and cultured in Ham's F12K (Gibco) plus 10% fetal bovine serum and 1% penicillin/streptomycin solution. All cells were used between passages 5 and 25 from receipt. Cells were seeded onto glass coverslips and transfected with EPAC-based cAMP indicator mTurq2Δ_Epac(CD,ΔDEP, Q270E)_td^{cp173}Ven (also known as EPAC-S^{H187} (86)), PKA indicator AKAR-4 (91), Ca^{2+} indicator GCamP6S (79), or cAMP indicator Flamindo2 (90) using Lipofectamine 3000 according to the manufacturer's instructions. FRET constructs were imaged using a CFP/YFP ratiometric filter set (Chroma Technologies, Bellows Falls, VT) on an IX-83 microscope (Olympus Life Sciences, Tokyo, Japan) equipped with a 30× (1.05 NA) silicone oil immersion objective as described previously (31, 127). NCI-H292 cells co-transfected with GCaMP6s, Flamindo2, or EPAC-S^{H187} and shRNAs were imaged 72 h after transfection using Micro-Manger/ImageJ (129) on an inverted microscope (Nikon, Tokyo Japan) with a 10× (0.45 NA) objective, XCite 110 LED light source (Excelitas Technologies, Waltham, MA), GFP filter cube (Chroma), and Photometrics Cool Snap HQ cooled interline CCD camera (Roper Scientific, Tucson, AZ). Due to the low transfection efficiencies of more differentiated epithelial cells (<10–15% for H292) and the fact that we were imaging responses in single transfected cells identified by fluorescent co-transfected proteins, we did not quantify the level of knockdown, as the population average would grossly underestimate knockdown due to the high percentage of untransfected cells.

Generation of primary sinonasal ALI cultures

All procedures were performed in accordance with the University of Pennsylvania School of Medicine guidelines regarding residual clinical material in research, the United States Department of Health and Human Services code of federal regulations Title 45 CFR 46.116, and the Declaration of Helsinki. Patients undergoing medically indicated sinonasal surgery were recruited from the Department of Otorhinolaryngology at the University of Pennsylvania with full institutional review board approval (approval no. 800614) and written informed consent. Inclusion criteria were patients ≥18 years of age undergoing sinonasal surgery for sinonasal disease (chronic rhinosinusitis) or other procedures (*e.g.* trans-nasal approaches to the skull base), in which tissue was classified as "control." Exclusion criteria included history of systemic inheritable disease (*e.g.* granulomatosis with polyangiitis, cystic fibrosis, systemic immunodeficiencies) or use of antibiotics, oral corticosteroids, or anti-biologics (*e.g.* Xolair) within 1 month of surgery. Members of vulnerable populations (*e.g.* individuals ≤18 years of age, pregnant women, cognitively impaired persons) were not included. Human sinonasal epithelial cells were enzymatically dissociated and grown to confluence in proliferation medium consisting of 50% Dulbecco's modified Eagle's medium/Ham's F-12 plus 50% bronchial epithelial basal medium (Lonza, Walkersville, MD) for 7 days (12, 130). Cells were then dissociated and seeded on porous polyester membranes coated with BSA, type I bovine collagen, and fibronectin in cell culture inserts. Culture medium was removed from the upper compartment, and basolateral medium was changed to differentiation medium (1:1 Dulbecco's modified Eagle's medium/bronchial epithelial basal medium) containing human epidermal growth factor (0.5 ng/ml), epinephrine (5 ng/ml), bovine pituitary extract (0.13 mg/ml), hydrocortisone (0.5 ng/ml), insulin (5 ng/ml), triiodothyronine (6.5 ng/ml), and transferrin (0.5 ng/ml), supplemented with 100 units/ml penicillin, 100 μg/ml streptomycin, 0.1 nM retinoic acid, and 2% NuSerum (BD Biosciences, San Jose, CA) as described previously (12, 130).

Live cell imaging of $[Ca^{2+}]_i$ and RNS production

All imaging experiments were carried out in HEPES-buffered HBSS. $[Ca^{2+}]_i$ and RNS were imaged using Fura-2 or Fluo-4 and DAF-FM, respectively, as described previously (12, 14, 15, 31, 131). For Ca^{2+} imaging of submerged airway cell lines, cells seeded on coverslips were loaded with fura-2/AM (2 μM) for 45 min at room temperature followed by a 20-min incubation in the dark. HEK293T cells were loaded with fura-2/AM (5 μM) for 75 min at room temperature. Primary sinonasal ALIs were loaded with fura-2/AM (5 μM applied apically) for 90 min, followed by washing and a 20-min incubation in the dark. ALIs were similarly loaded with 10 μM DAF-FM diacetate for 90 min in the presence of 5 μM carboxy-PTIO, followed by washing to

remove unloaded DAF-FM and cPTIO and incubation for 15 min before imaging. Because of potential toxicity issues related to AM-ester–based dyes (*e.g.* formaldehyde release from de-esterification, reactive oxygen species production from illumination, Ca^{2+} chelation), care was taken to minimize dye loading as well as sample illumination using neutral density filters to minimize excitation light, increasing camera sensitivity with pixel binning, and minimizing sampling frequency (1 frame every 4 or 8 s for most experiments) using established loading and illumination protocols (12, 31, 101, 108, 132–134).

Imaging of ALIs was performed using an Olympus IX-83 microscope (10×, 0.4 NA PlanApo objective) equipped with a fluorescence xenon lamp (Sutter Lambda LS, Sutter Instruments, Novato, CA), excitation and emission filter wheels (Sutter Instruments), and a 16-bit Hamamatsu Orca Flash 4.0 sCMOS camera. Images were acquired and analyzed using MetaFluor (Molecular Devices, Sunnyvale, CA). For fura-2 $[Ca^{2+}]_i$ measurement in submerged cells, either a 20× (0.8 NA; UPLNAPO) air or 30× (1.05 NA; UPLSAPO) silicone immersion objective (Olympus) using MetaFluor. Due to potential errors and/or enhanced variability (*e.g.* (135)) introduced with calibration of ratios to $[Ca^{2+}]_i$ and the fact that the comparisons made here did not necessitate absolute measure of $[Ca^{2+}]_i$, we report most data as 340/380 excitation ratio rather than calibrated $[Ca^{2+}]_i$. Calibration of fura-2 fluorescence into estimates of global $[Ca^{2+}]_i$ was carried out in primary cells as described previously (31, 108, 133) to illustrate the magnitude of T2R *versus* purinergic $[Ca^{2+}]_i$ signals. However, fura-2 calibration represents global $[Ca^{2+}]_i$ and does not provide information about localized concentrations that may occur (136) (*e.g.* within cilia (137) or in the vicinity of NOS enzymes (138)).

Whereas different objectives were used to acquire different fura-2 data sets in this study, only data acquired with the same objective are compared. Data in Fig. 1 were imaged at 20×, data in Figs. 2 and 3 were imaged at 30×, and data in Fig. 8 were imaged at 10×, as a longer working distance was required for imaging through transwell filters. DAF-FM measurements utilized raw fluorescence values to compare experiments performed under identical conditions with identical microscope settings.

Measurement of NO_2^-/NO_3^- and cAMP in primary sinonasal ALIs

A fluorometric NO_2^-/NO_3^- kit (Cayman Chemical, Ann Arbor, MI) was used, and measurements were carried out according to the manufacturer's instructions. ALIs were changed to basolateral medium lacking phenol red and serum and treated with agonist as indicated in 30 μl of apical PBS. Apical solution was collected after 18 h and assayed for total NO_2^-/NO_3^-. For cAMP measurements, primary sinonasal ALIs were transferred to basolateral HBSS and stimulated with agonists as indicated in 30 μl of apical HBSS. After 10 min, cells were lysed and assayed for cAMP using the Amersham Biosciences cAMP Biotrak Enzyme Immunoassay System (GE Healthcare) according to the manufacturer's instructions.

Immunofluorescence microscopy

Immunofluorescence microscopy was carried out as described previously (12), with modifications outlined below. ALI cultures were fixed in 4% formaldehyde for 20 min at room temperature, followed by blocking and permeabilization in Dulbecco's PBS containing 1% BSA, 5% normal donkey serum, 0.2% saponin, and 0.3% Triton X-100 for 1 h at 4 °C. Primary antibody incubation (1:100 for anti-T2R antibodies, 1:250 for tubulin antibodies) was carried out at 4 °C overnight. Alexa Fluor–labeled donkey anti-mouse or rabbit secondary antibody incubation (1:1000) was carried out for 2 h at 4 °C. Transwell filters were removed from the plastic mounting ring and mounted with Fluoroshield with 4′,6-diamidino-2-phenylindole (Abcam). For direct labeling of primary antibodies to colocalize T2R38 and T2R16, Zenon antibody labeling kits (Thermo Scientific) were used according to the manufacturer's instructions. Images of ALIs were taken on an Olympus Fluoview confocal system with an IX-81 microscope and 60× (1.4 NA) objective. Acceptor bleaching experiments were carried out using the tornado bleaching function in Fluoview software. Images were analyzed using Fluoview software and/or the FIJI (139) version of ImageJ (W. Rasband, Research Services Branch, NIMH, National Institutes of Health, Bethesda, MD).

Genotyping of patient samples and ALI cultures

Genomic DNA was extracted from cultured cells or sinonasal specimens following the directions of the manufacturer (QIAamp DNA Mini kit and Blood Mini kit; Qiagen). Following extraction, samples were quantified using a spectrophotometer (ND-1000, Nanodrop), using 1.5 μl of extracted genomic DNA. Samples were diluted to 5 ng/μl and genotyped using the ABI StepOne real-time PCR system. Alleles of the *TAS2R38* gene were genotyped for a variant site using allele-specific probes and primers (Applied Biosystems).

Data analysis and statistics

One-way analysis of variance (ANOVA) was performed in GraphPad Prism with appropriate post-tests as indicated; $p < 0.05$ was considered statistically significant. For comparisons of all samples within a data set, Tukey–Kramer post-test was used. For preselected pairwise comparisons, Bonferroni post-test was performed. For comparisons with a single control group, Dunnett's post-test was used. All other data analysis was performed in Excel. For all figures, one asterisk or number sign (* or #) indicates $p < 0.05$, and two (** or ##) indicate $p < 0.01$, respectively; *n.s.* indicates no statistical significance. All data are presented as mean ± S.E. Data values from bar graphs are given in the supporting information.

Author contributions—J. R. F. and R. J. L. performed experiments. L. J. D., N. D. A., J. N. P., and D. W. K. recruited patients, aided with tissue procurement and regulatory approvals, cultured primary human cells, maintained clinical databases and records, and intellectually contributed. C. J. M., D. R. R., and P. J. contributed critical reagents and expertise for heterologous expression (P. J.) and patient sample genotyping (C. J. M. and D. R. R.) as well as intellectual discussion and interpretation. J. R. F. and R. J. L. designed the study, analyzed data, and wrote the paper. All authors reviewed and approved the manuscript.

Acknowledgments—We thank J. B. Klarenbeek and K. Jalink (Netherlands Cancer Institute) for EPAC-S^{H187} construct, B. Chen (University of Pennsylvania) for assistance with ALI cultures, and M. Victoria and D. B. McMahon (University of Pennsylvania) for excellent technical assistance throughout the study.

References

1. Blalock, J. E. (2005) The immune system as the sixth sense. *J. Intern. Med.* **257,** 126–138 CrossRef Medline
2. Blalock, J. E., and Smith, E. M. (2007) Conceptual development of the immune system as a sixth sense. *Brain Behav. Immun.* **21,** 23–33 CrossRef Medline
3. Bedford, F. L. (2011) The missing sense modality: the immune system. *Perception* **40,** 1265–1267 CrossRef Medline
4. Weigent, D. A., and Blalock, J. E. (1995) Associations between the neuroendocrine and immune systems. *J. Leukoc. Biol.* **58,** 137–150 CrossRef Medline
5. Ferencík, M., and Stvrtinová, V. (1997) [Is the immune system our sixth sense? Relation between the immune and neuroendocrine systems]. *Bratisl. Lek. Listy* **98,** 187–198 Medline
6. Li, F. (2013) Taste perception: from the tongue to the testis. *Mol. Hum. Reprod.* **19,** 349–360 CrossRef Medline
7. Yamamoto, K., and Ishimaru, Y. (2013) Oral and extra-oral taste perception. *Semin. Cell Dev. Biol.* **24,** 240–246 CrossRef Medline
8. An, S. S., and Liggett, S. B. (2018) Taste and smell GPCRs in the lung: evidence for a previously unrecognized widespread chemosensory system. *Cell. Signal.* **41,** 82–88 Medline
9. Lee, R. J., and Cohen, N. A. (2015) Taste receptors in innate immunity. *Cell. Mol. Life Sci.* **72,** 217–236 CrossRef Medline
10. Shah, A. S., Ben-Shahar, Y., Moninger, T. O., Kline, J. N., and Welsh, M. J. (2009) Motile cilia of human airway epithelia are chemosensory. *Science* **325,** 1131–1134 CrossRef Medline
11. Clark, A. A., Liggett, S. B., and Munger, S. D. (2012) Extraoral bitter taste receptors as mediators of off-target drug effects. *FASEB J.* **26,** 4827–4831 CrossRef Medline
12. Lee, R. J., Xiong, G., Kofonow, J. M., Chen, B., Lysenko, A., Jiang, P., Abraham, V., Doghramji, L., Adappa, N. D., Palmer, J. N., Kennedy, D. W., Beauchamp, G. K., Doulias, P.-T., Ischiropoulos, H., Kreindler, J. L., *et al.* (2012) T2R38 taste receptor polymorphisms underlie susceptibility to upper respiratory infection. *J. Clin. Invest.* **122,** 4145–4159 CrossRef Medline
13. Lee, R. J., and Cohen, N. A. (2015) Role of the bitter taste receptor T2R38 in upper respiratory infection and chronic rhinosinusitis. *Curr. Opin. Allergy Clin. Immunol.* **15,** 14–20 CrossRef Medline
14. Lee, R. J., Chen, B., Redding, K. M., Margolskee, R. F., and Cohen, N. A. (2014) Mouse nasal epithelial innate immune responses to *Pseudomonas aeruginosa* quorum-sensing molecules require taste signaling components. *Innate Immun.* **20,** 606–617 CrossRef Medline
15. Lee, R. J., Kofonow, J. M., Rosen, P. L., Siebert, A. P., Chen, B., Doghramji, L., Xiong, G., Adappa, N. D., Palmer, J. N., Kennedy, D. W., Kreindler, J. L., Margolskee, R. F., and Cohen, N. A. (2014) Bitter and sweet taste receptors regulate human upper respiratory innate immunity. *J. Clin. Invest.* **124,** 1393–1405 CrossRef Medline
16. Lee, R. J., and Cohen, N. A. (2014) Bitter and sweet taste receptors in the respiratory epithelium in health and disease. *J. Mol. Med.* **92,** 1235–1244 CrossRef Medline
17. Lee, R. J., and Cohen, N. A. (2013) The emerging role of the bitter taste receptor T2R38 in upper respiratory infection and chronic rhinosinusitis. *Am. J. Rhinol. Allergy* **27,** 283–286 CrossRef Medline
18. Workman, A. D., Carey, R. M., Kohanski, M. A., Kennedy, D. W., Palmer, J. N., Adappa, N. D., and Cohen, N. A. (2017) Relative susceptibility of airway organisms to antimicrobial effects of nitric oxide. *Int. Forum Allergy Rhinol.* **7,** 770–776 CrossRef Medline
19. Marcinkiewicz, J. (1997) Nitric oxide and antimicrobial activity of reactive oxygen intermediates. *Immunopharmacology* **37,** 35–41 CrossRef Medline
20. Fang, F. C. (1997) Perspectives series: host/pathogen interactions: mechanisms of nitric oxide-related antimicrobial activity. *J. Clin. Invest.* **99,** 2818–2825 CrossRef Medline
21. Stevens, W. W., Lee, R. J., Schleimer, R. P., and Cohen, N. A. (2015) Chronic rhinosinusitis pathogenesis. *J. Allergy Clin. Immunol.* **136,** 1442–1453 CrossRef Medline
22. Bufe, B., Breslin, P. A., Kuhn, C., Reed, D. R., Tharp, C. D., Slack, J. P., Kim, U. K., Drayna, D., and Meyerhof, W. (2005) The molecular basis of individual differences in phenylthiocarbamide and propylthiouracil bitterness perception. *Curr. Biol.* **15,** 322–327 CrossRef Medline
23. Adappa, N. D., Truesdale, C. M., Workman, A. D., Doghramji, L., Mansfield, C., Kennedy, D. W., Palmer, J. N., Cowart, B. J., and Cohen, N. A. (2016) Correlation of T2R38 taste phenotype and *in vitro* biofilm formation from nonpolypoid chronic rhinosinusitis patients. *Int. Forum Allergy Rhinol.* **6,** 783–791 CrossRef Medline
24. Rom, D. I., Christensen, J. M., Alvarado, R., Sacks, R., and Harvey, R. J. (2017) The impact of bitter taste receptor genetics on culturable bacteria in chronic rhinosinusitis. *Rhinology* **55,** 90–94 Medline
25. Cantone, E., Negri, R., Roscetto, E., Grassia, R., Catania, M. R., Capasso, P., Maffei, M., Soriano, A. A., Leone, C. A., Iengo, M., and Greco, L. (2018) *In vivo* biofilm formation, Gram-negative infections and TAS2R38 polymorphisms in CRSw NP patients. *Laryngoscope* CrossRef
26. Adappa, N. D., Zhang, Z., Palmer, J. N., Kennedy, D. W., Doghramji, L., Lysenko, A., Reed, D. R., Scott, T., Zhao, N. W., Owens, D., Lee, R. J., and Cohen, N. A. (2014) The bitter taste receptor T2R38 is an independent risk factor for chronic rhinosinusitis requiring sinus surgery. *Int. Forum Allergy Rhinol.* **4,** 3–7 CrossRef Medline
27. Adappa, N. D., Howland, T. J., Palmer, J. N., Kennedy, D. W., Doghramji, L., Lysenko, A., Reed, D. R., Lee, R. J., and Cohen, N. A. (2013) Genetics of the taste receptor T2R38 correlates with chronic rhinosinusitis necessitating surgical intervention. *Int. Forum Allergy Rhinol.* **3,** 184–187 CrossRef Medline
28. Mfuna Endam, L., Filali-Mouhim, A., Boisvert, P., Boulet, L. P., Bossé, Y., and Desrosiers, M. (2014) Genetic variations in taste receptors are associated with chronic rhinosinusitis: a replication study. *Int. Forum Allergy Rhinol.* **4,** 200–206 CrossRef Medline
29. Dzaman, K., Zagor, M., Sarnowska, E., Krzeski, A., and Kantor, I. (2016) The correlation of TAS2R38 gene variants with higher risk for chronic rhinosinusitis in Polish patients. *Otolaryngol. Pol.* **70,** 13–18 CrossRef Medline
30. Adappa, N. D., Farquhar, D., Palmer, J. N., Kennedy, D. W., Doghramji, L., Morris, S. A., Owens, D., Mansfield, C., Lysenko, A., Lee, R. J., Cowart, B. J., Reed, D. R., and Cohen, N. A. (2016) TAS2R38 genotype predicts surgical outcome in nonpolypoid chronic rhinosinusitis. *Int. Forum Allergy Rhinol.* **6,** 25–33 Medline
31. Hariri, B. M., McMahon, D. B., Chen, B., Freund, J. R., Mansfield, C. J., Doghramji, L. J., Adappa, N. D., Palmer, J. N., Kennedy, D. W., Reed, D. R., Jiang, P., and Lee, R. J. (2017) Flavones modulate respiratory epithelial innate immunity: anti-inflammatory effects and activation of the T2R14 receptor. *J. Biol. Chem.* **292,** 8484–8497 CrossRef Medline
32. Yan, C. H., Hahn, S., McMahon, D., Bonislawski, D., Kennedy, D. W., Adappa, N. D., Palmer, J. N., Jiang, P., Lee, R. J., and Cohen, N. A. (2017) Nitric oxide production is stimulated by bitter taste receptors ubiquitously expressed in the sinonasal cavity. *Am. J. Rhinol. Allergy* **31,** 85–92 CrossRef Medline
33. Paczkowski, J. E., Mukherjee, S., McCready, A. R., Cong, J. P., Aquino, C. J., Kim, H., Henke, B. R., Smith, C. D., and Bassler, B. L. (2017) Flavonoids suppress *Pseudomonas aeruginosa* virulence through allosteric inhibition of quorum-sensing receptors. *J. Biol. Chem.* **292,** 4064–4076 CrossRef Medline
34. Jimenez, P. N., Koch, G., Thompson, J. A., Xavier, K. B., Cool, R. H., and Quax, W. J. (2012) The multiple signaling systems regulating virulence in Pseudomonas aeruginosa. *Microbiol. Mol. Biol. Rev.* **76,** 46–65 CrossRef Medline
35. McGrath, S., Wade, D. S., and Pesci, E. C. (2004) Dueling quorum sensing systems in *Pseudomonas aeruginosa* control the production of the *Pseudomonas quinolone* signal (PQS). *FEMS Microbiol. Lett.* **230,** 27–34

CrossRef Medline
36. Pearson, J. P., Pesci, E. C., and Iglewski, B. H. (1997) Roles of *Pseudomonas aeruginosa* las and rhl quorum-sensing systems in control of elastase and rhamnolipid biosynthesis genes. *J. Bacteriol.* **179,** 5756–5767 CrossRef Medline
37. Heeb, S., Fletcher, M. P., Chhabra, S. R., Diggle, S. P., Williams, P., and Cámara, M. (2011) Quinolones: from antibiotics to autoinducers. *FEMS Microbiol. Rev.* **35,** 247–274 CrossRef Medline
38. Dubern, J. F., and Diggle, S. P. (2008) Quorum sensing by 2-alkyl-4-quinolones in *Pseudomonas aeruginosa* and other bacterial species. *Mol. Biosyst.* **4,** 882–888 CrossRef Medline
39. Diggle, S. P., Cornelis, P., Williams, P., and Cámara, M. (2006) 4-Quinolone signalling in *Pseudomonas aeruginosa*: old molecules, new perspectives. *Int. J. Med. Microbiol.* **296,** 83–91 CrossRef Medline
40. Kanthakumar, K., Taylor, G., Tsang, K. W., Cundell, D. R., Rutman, A., Smith, S., Jeffery, P. K., Cole, P. J., and Wilson, R. (1993) Mechanisms of action of *Pseudomonas aeruginosa* pyocyanin on human ciliary beat *in vitro*. *Infect. Immun.* **61,** 2848–2853 Medline
41. Wilson, R., Pitt, T., Taylor, G., Watson, D., MacDermot, J., Sykes, D., Roberts, D., and Cole, P. (1987) Pyocyanin and 1-hydroxyphenazine produced by *Pseudomonas aeruginosa* inhibit the beating of human respiratory cilia *in vitro*. *J. Clin. Invest.* **79,** 221–229 CrossRef Medline
42. Hingley, S. T., Hastie, A. T., Kueppers, F., Higgins, M. L., Weinbaum, G., and Shryock, T. (1986) Effect of ciliostatic factors from *Pseudomonas aeruginosa* on rabbit respiratory cilia. *Infect. Immun.* **51,** 254–262 Medline
43. Denning, G. M., Wollenweber, L. A., Railsback, M. A., Cox, C. D., Stoll, L. L., and Britigan, B. E. (1998) *Pseudomonas* pyocyanin increases interleukin-8 expression by human airway epithelial cells. *Infect. Immun.* **66,** 5777–5784 Medline
44. Oliphant, C. M., and Green, G. M. (2002) Quinolones: a comprehensive review. *Am. Fam. Physician* **65,** 455–464 Medline
45. Meyerhof, W., Batram, C., Kuhn, C., Brockhoff, A., Chudoba, E., Bufe, B., Appendino, G., and Behrens, M. (2010) The molecular receptive ranges of human TAS2R bitter taste receptors. *Chem. Senses* **35,** 157–170 CrossRef Medline
46. Lossow, K., Hübner, S., Roudnitzky, N., Slack, J. P., Pollastro, F., Behrens, M., and Meyerhof, W. (2016) Comprehensive analysis of mouse bitter taste receptors reveals different molecular receptive ranges for orthologous receptors in mice and humans. *J. Biol. Chem.* **291,** 15358–15377 CrossRef Medline
47. Levit, A., Nowak, S., Peters, M., Wiener, A., Meyerhof, W., Behrens, M., and Niv, M. Y. (2014) The bitter pill: clinical drugs that activate the human bitter taste receptor TAS2R14. *FASEB J.* **28,** 1181–1197 CrossRef Medline
48. Tipton, K. A., Coleman, J. P., and Pesci, E. C. (2015) Post-transcriptional regulation of gene PA5507 controls *Pseudomonas* quinolone signal concentration in *P. aeruginosa*. *Mol. Microbiol.* **96,** 670–683 CrossRef Medline
49. Häussler, S., and Becker, T. (2008) The *Pseudomonas* quinolone signal (PQS) balances life and death in *Pseudomonas aeruginosa* populations. *PLoS Pathog.* **4,** e1000166 CrossRef Medline
50. Diggle, S. P., Matthijs, S., Wright, V. J., Fletcher, M. P., Chhabra, S. R., Lamont, I. L., Kong, X., Hider, R. C., Cornelis, P., Cámara, M., and Williams, P. (2007) The *Pseudomonas aeruginosa* 4-quinolone signal molecules HHQ and PQS play multifunctional roles in quorum sensing and iron entrapment. *Chem. Biol.* **14,** 87–96 CrossRef Medline
51. Lin, J., Zhang, W., Cheng, J., Yang, X., Zhu, K., Wang, Y., Wei, G., Qian, P. Y., Luo, Z. Q., and Shen, X. (2017) A *Pseudomonas* T6SS effector recruits PQS-containing outer membrane vesicles for iron acquisition. *Nat. Commun.* **8,** 14888 CrossRef Medline
52. Hotterbeekx, A., Kumar-Singh, S., Goossens, H., and Malhotra-Kumar, S. (2017) *In vivo* and *in vitro* Interactions between *Pseudomonas aeruginosa* and *Staphylococcus* spp. *Front. Cell Infect. Microbiol.* **7,** 106 Medline
53. Liu, Y. C., Chan, K. G., and Chang, C. Y. (2015) Modulation of host biology by *Pseudomonas aeruginosa* quorum sensing signal molecules: messengers or traitors. *Front. Microbiol.* **6,** 1226 Medline
54. Guina, T., Purvine, S. O., Yi, E. C., Eng, J., Goodlett, D. R., Aebersold, R., and Miller, S. I. (2003) Quantitative proteomic analysis indicates increased synthesis of a quinolone by *Pseudomonas aeruginosa* isolates from cystic fibrosis airways. *Proc. Natl. Acad. Sci. U.S.A.* **100,** 2771–2776 CrossRef Medline
55. Abdalla, M. Y., Hoke, T., Seravalli, J., Switzer, B. L., Bavitz, M., Fliege, J. D., Murphy, P. J., and Britigan, B. E. (2017) *Pseudomonas* quinolone signal induces oxidative stress and inhibits heme oxygenase-1 expression in lung epithelial cells. *Infect. Immun.* **85,** e00176-17 Medline
56. Morales-Soto, N., Dunham, S. J. B., Baig, N. F., Ellis, J. F., Madukoma, C. S., Bohn, P. W., Sweedler, J. V., and Shrout, J. D. (2018) Spatially-dependent alkyl quinolone signaling responses to antibiotics in *Pseudomonas aeruginosa* swarms. *J. Biol. Chem.* **293,** 9544–9552
57. Langan, K. M., Kotsimbos, T., and Peleg, A. Y. (2015) Managing *Pseudomonas aeruginosa* respiratory infections in cystic fibrosis. *Curr. Opin. Infect. Dis.* **28,** 547–556 Medline
58. Reen, F. J., Mooij, M. J., Holcombe, L. J., McSweeney, C. M., McGlacken, G. P., Morrissey, J. P., and O'Gara, F. (2011) The *Pseudomonas* quinolone signal (PQS), and its precursor HHQ, modulate interspecies and interkingdom behaviour. *FEMS Microbiol. Ecol.* **77,** 413–428 CrossRef Medline
59. Ha, D. G., Merritt, J. H., Hampton, T. H., Hodgkinson, J. T., Janecek, M., Spring, D. R., Welch, M., and O'Toole, G. A. (2011) 2-Heptyl-4-quinolone, a precursor of the *Pseudomonas quinolone* signal molecule, modulates swarming motility in *Pseudomonas aeruginosa*. *J. Bacteriol.* **193,** 6770–6780 CrossRef Medline
60. Gruber, J. D., Chen, W., Parnham, S., Beauchesne, K., Moeller, P., Flume, P. A., and Zhang, Y. M. (2016) The role of 2,4-dihydroxyquinoline (DHQ) in *Pseudomonas aeruginosa* pathogenicity. *PeerJ* **4,** e1495 CrossRef Medline
61. Fulcher, M. L., and Randell, S. H. (2013) Human nasal and tracheobronchial respiratory epithelial cell culture. *Methods Mol. Biol.* **945,** 109–121 Medline
62. Woodworth, B. A., Antunes, M. B., Bhargave, G., Palmer, J. N., and Cohen, N. A. (2007) Murine tracheal and nasal septal epithelium for air-liquid interface cultures: a comparative study. *Am. J. Rhinol.* **21,** 533–537 CrossRef Medline
63. Dimova, S., Brewster, M. E., Noppe, M., Jorissen, M., and Augustijns, P. (2005) The use of human nasal *in vitro* cell systems during drug discovery and development. *Toxicol. In Vitro* **19,** 107–122 CrossRef Medline
64. Huang, W., Shen, Q., Su, X., Ji, M., Liu, X., Chen, Y., Lu, S., Zhuang, H., and Zhang, J. (2016) BitterX: a tool for understanding bitter taste in humans. *Sci. Rep.* **6,** 23450 CrossRef Medline
65. Mody, S. M., Ho, M. K., Joshi, S. A., and Wong, Y. H. (2000) Incorporation of Gα(z)-specific sequence at the carboxyl terminus increases the promiscuity of Gα(16) toward G(i)-coupled receptors. *Mol. Pharmacol.* **57,** 13–23 Medline
66. Liu, A. M., Ho, M. K., Wong, C. S., Chan, J. H., Pau, A. H., and Wong, Y. H. (2003) Gα(16/z) chimeras efficiently link a wide range of G protein-coupled receptors to calcium mobilization. *J. Biomol. Screen.* **8,** 39–49 CrossRef Medline
67. Behrens, M., Gu, M., Fan, S., Huang, C., and Meyerhof, W. (2018) Bitter substances from plants used in traditional Chinese medicine exert biased activation of human bitter taste receptors. *Chem. Biol. Drug Des.* **91,** 422–433 Medline
68. Calfee, M. W., Shelton, J. G., McCubrey, J. A., and Pesci, E. C. (2005) Solubility and bioactivity of the *Pseudomonas* quinolone signal are increased by a *Pseudomonas* aeruginosa-produced surfactant. *Infect. Immun.* **73,** 878–882 CrossRef Medline
69. Pydi, S. P., Sobotkiewicz, T., Billakanti, R., Bhullar, R. P., Loewen, M. C., and Chelikani, P. (2014) Amino acid derivatives as bitter taste receptor (T2R) blockers. *J. Biol. Chem.* **289,** 25054–25066 CrossRef Medline
70. Greene, T. A., Alarcon, S., Thomas, A., Berdougo, E., Doranz, B. J., Breslin, P. A., and Rucker, J. B. (2011) Probenecid inhibits the human bitter taste receptor TAS2R16 and suppresses bitter perception of salicin. *PLoS One* **6,** e20123 CrossRef Medline
71. Adappa, N. D., Workman, A. D., Hadjiliadis, D., Dorgan, D. J., Frame, D., Brooks, S., Doghramji, L., Palmer, J. N., Mansfield, C., Reed, D. R., and Cohen, N. A. (2016) T2R38 genotype is correlated with sinonasal quality

of life in homozygous ΔF508 cystic fibrosis patients. *Int. Forum Allergy Rhinol.* **6,** 356–361 CrossRef Medline
72. Wen, X., Zhou, J., Zhang, D., Li, J., Wang, Q., Feng, N., Zhu, H., Song, Y., Li, H., and Bai, C. (2015) Denatonium inhibits growth and induces apoptosis of airway epithelial cells through mitochondrial signaling pathways. *Respir. Res.* **16,** 13 CrossRef Medline
73. Kim, D., Pauer, S. H., Yong, H. M., An, S. S., and Liggett, S. B. (2016) β_2-Adrenergic receptors chaperone trapped bitter taste receptor 14 to the cell surface as a heterodimer and exert unidirectional desensitization of taste receptor function. *J. Biol. Chem.* **291,** 17616–17628 CrossRef Medline
74. Miyamoto, S., Izumi, M., Hori, M., Kobayashi, M., Ozaki, H., and Karaki, H. (2000) Xestospongin C, a selective and membrane-permeable inhibitor of IP(3) receptor, attenuates the positive inotropic effect of α-adrenergic stimulation in guinea-pig papillary muscle. *Br. J. Pharmacol.* **130,** 650–654 CrossRef Medline
75. Lehmann, D. M., Seneviratne, A. M., and Smrcka, A. V. (2008) Small molecule disruption of G protein βγ subunit signaling inhibits neutrophil chemotaxis and inflammation. *Mol. Pharmacol.* **73,** 410–418 Medline
76. Zhang, C. H., Lifshitz, L. M., Uy, K. F., Ikebe, M., Fogarty, K. E., and ZhuGe, R. (2013) The cellular and molecular basis of bitter tastant-induced bronchodilation. *PLoS Biol.* **11,** e1001501 CrossRef Medline
77. Deshpande, D. A., Wang, W. C., McIlmoyle, E. L., Robinett, K. S., Schillinger, R. M., An, S. S., Sham, J. S., and Liggett, S. B. (2010) Bitter taste receptors on airway smooth muscle bronchodilate by localized calcium signaling and reverse obstruction. *Nat. Med.* **16,** 1299–1304 CrossRef Medline
78. Tan, X., and Sanderson, M. J. (2014) Bitter tasting compounds dilate airways by inhibiting airway smooth muscle calcium oscillations and calcium sensitivity. *Br. J. Pharmacol.* **171,** 646–662 CrossRef Medline
79. Chen, T. W., Wardill, T. J., Sun, Y., Pulver, S. R., Renninger, S. L., Baohan, A., Schreiter, E. R., Kerr, R. A., Orger, M. B., Jayaraman, V., Looger, L. L., Svoboda, K., and Kim, D. S. (2013) Ultrasensitive fluorescent proteins for imaging neuronal activity. *Nature* **499,** 295–300 CrossRef Medline
80. Wong, G. T., Gannon, K. S., and Margolskee, R. F. (1996) Transduction of bitter and sweet taste by gustducin. *Nature* **381,** 796–800 CrossRef Medline
81. Hoon, M. A., Northup, J. K., Margolskee, R. F., and Ryba, N. J. (1995) Functional expression of the taste specific G-protein, α-gustducin. *Biochem. J.* **309,** 629–636 CrossRef Medline
82. McLaughlin, S. K., McKinnon, P. J., Spickofsky, N., Danho, W., and Margolskee, R. F. (1994) Molecular cloning of G proteins and phosphodiesterases from rat taste cells. *Physiol. Behav.* **56,** 1157–1164 CrossRef Medline
83. McLaughlin, S. K., McKinnon, P. J., and Margolskee, R. F. (1992) Gustducin is a taste-cell-specific G protein closely related to the transducins. *Nature* **357,** 563–569 CrossRef Medline
84. Cohen, S. P., Buckley, B. K., Kosloff, M., Garland, A. L., Bosch, D. E., Cheng, G., Jr., Radhakrishna, H., Brown, M. D., Willard, F. S., Arshavsky, V. Y., Tarran, R., Siderovski, D. P., and Kimple, A. J. (2012) Regulator of G-protein signaling-21 (RGS21) is an inhibitor of bitter gustatory signaling found in lingual and airway epithelia. *J. Biol. Chem.* **287,** 41706–41719 CrossRef Medline
85. Kim, D., Woo, J. A., Geffken, E., An, S. S., and Liggett, S. B. (2017) Coupling of airway smooth muscle bitter taste receptors to intracellular signaling and relaxation is via Gαi1,2,3. *Am. J. Respir. Cell Mol. Biol.* **56,** 762–771 CrossRef Medline
86. Klarenbeek, J., Goedhart, J., van Batenburg, A., Groenewald, D., and Jalink, K. (2015) Fourth-generation epac-based FRET sensors for cAMP feature exceptional brightness, photostability and dynamic range: characterization of dedicated sensors for FLIM, for ratiometry and with high affinity. *PLoS One* **10,** e0122513 CrossRef Medline
87. Storch, U., Straub, J., Erdogmus, S., Gudermann, T., and Mederos Y. Schnitzler, M. (2017) Dynamic monitoring of $G_{i/o}$-protein-mediated decreases of intracellular cAMP by FRET-based Epac sensors. *Pflugers Arch.* **469,** 725–737 CrossRef Medline
88. Mangmool, S., and Kurose, H. (2011) G(i/o) protein-dependent and -independent actions of pertussis toxin (PTX). *Toxins* **3,** 884–899 CrossRef Medline
89. Ozeck, M., Brust, P., Xu, H., and Servant, G. (2004) Receptors for bitter, sweet and umami taste couple to inhibitory G protein signaling pathways. *Eur. J. Pharmacol.* **489,** 139–149 CrossRef Medline
90. Odaka, H., Arai, S., Inoue, T., and Kitaguchi, T. (2014) Genetically-encoded yellow fluorescent cAMP indicator with an expanded dynamic range for dual-color imaging. *PLoS One* **9,** e100252 CrossRef Medline
91. Depry, C., Allen, M. D., and Zhang, J. (2011) Visualization of PKA activity in plasma membrane microdomains. *Mol. Biosyst.* **7,** 52–58 CrossRef Medline
92. Violin, J. D., Zhang, J., Tsien, R. Y., and Newton, A. C. (2003) A genetically encoded fluorescent reporter reveals oscillatory phosphorylation by protein kinase C. *J. Cell Biol.* **161,** 899–909 CrossRef Medline
93. König, P., Krasteva, G., Tag, C., König, I. R., Arens, C., and Kummer, W. (2006) FRET-CLSM and double-labeling indirect immunofluorescence to detect close association of proteins in tissue sections. *Lab. Invest.* **86,** 853–864 CrossRef Medline
94. Reed, D. R., Zhu, G., Breslin, P. A., Duke, F. F., Henders, A. K., Campbell, M. J., Montgomery, G. W., Medland, S. E., Martin, N. G., and Wright, M. J. (2010) The perception of quinine taste intensity is associated with common genetic variants in a bitter receptor cluster on chromosome 12. *Hum. Mol. Genet.* **19,** 4278–4285 CrossRef Medline
95. Workman, A. D., Maina, I. W., Brooks, S. G., Kohanski, M. A., Cowart, B. J., Mansfield, C., Kennedy, D. W., Palmer, J. N., Adappa, N. D., Reed, D. R., Lee, R. J., and Cohen, N. A. (2018) The role of quinine-responsive T2Rs in airway immune defense and chronic rhinosinusitis. *Front. Immunol.* **9,** 624 CrossRef Medline
96. Workman, A. D., Brooks, S. G., Kohanski, M. A., Blasetti, M. T., Cowart, B. J., Mansfield, C., Kennedy, D. W., Palmer, J. N., Adappa, N. D., Reed, D. R., and Cohen, N. A. (2018) Bitter and sweet taste tests are reflective of disease status in chronic rhinosinusitis. *J. Allergy Clin. Immunol. Pract.* **6,** 1078–1080 CrossRef Medline
97. Karaman, R., Nowak, S., Di Pizio, A., Kitaneh, H., Abu-Jaish, A., Meyerhof, W., Niv, M. Y., and Behrens, M. (2016) Probing the binding pocket of the broadly tuned human bitter taste receptor TAS2R14 by chemical modification of cognate agonists. *Chem. Biol. Drug Des.* **88,** 66–75 CrossRef Medline
98. Tan, J., Abrol, R., Trzaskowski, B., and Goddard, W. A., 3rd (2012) 3D structure prediction of TAS2R38 bitter receptors bound to agonists phenylthiocarbamide (PTC) and 6-*n*-propylthiouracil (PROP). *J. Chem. Inf. Model.* **52,** 1875–1885 CrossRef Medline
99. Thomas, A., Sulli, C., Davidson, E., Berdougo, E., Phillips, M., Puffer, B. A., Paes, C., Doranz, B. J., and Rucker, J. B. (2017) The bitter taste receptor TAS2R16 achieves high specificity and accommodates diverse glycoside ligands by using a two-faced binding pocket. *Sci. Rep.* **7,** 7753 CrossRef Medline
100. Verbeurgt, C., Veithen, A., Carlot, S., Tarabichi, M., Dumont, J. E., Hassid, S., and Chatelain, P. (2017) The human bitter taste receptor T2R38 is broadly tuned for bacterial compounds. *PLoS One* **12,** e0181302 CrossRef Medline
101. Lee, R. J., Chen, B., Doghramji, L., Adappa, N. D., Palmer, J. N., Kennedy, D. W., and Cohen, N. A. (2013) Vasoactive intestinal peptide regulates sinonasal mucociliary clearance and synergizes with histamine in stimulating sinonasal fluid secretion. *FASEB J.* **27,** 5094–5103 CrossRef Medline
102. Hariri, B. M., Payne, S. J., Chen, B., Mansfield, C., Doghramji, L. J., Adappa, N. D., Palmer, J. N., Kennedy, D. W., Niv, M. Y., and Lee, R. J. (2016) *In vitro* effects of anthocyanidins on sinonasal epithelial nitric oxide production and bacterial physiology. *Am. J. Rhinol. Allergy* **30,** 261–268 CrossRef Medline
103. Maurer, S., Wabnitz, G. H., Kahle, N. A., Stegmaier, S., Prior, B., Giese, T., Gaida, M. M., Samstag, Y., and Hänsch, G. M. (2015) Tasting *Pseudomonas aeruginosa* biofilms: human neutrophils express the bitter receptor T2R38 as sensor for the quorum sensing molecule *N*-(3-oxododecanoyl)-L-homoserine lactone. *Front. Immunol.* **6,** 369 Medline
104. Gaida, M. M., Dapunt, U., and Hänsch, G. M. (2016) Sensing developing biofilms: the bitter receptor T2R38 on myeloid cells. *Pathog. Dis.* **74,**

ftw004 CrossRef Medline
105. Sandau, M. M., Goodman, J. R., Thomas, A., Rucker, J. B., and Rawson, N. E. (2015) A functional comparison of the domestic cat bitter receptors Tas2r38 and Tas2r43 with their human orthologs. *BMC Neurosci.* **16,** 33 CrossRef Medline
106. Gaida, M. M., Mayer, C., Dapunt, U., Stegmaier, S., Schirmacher, P., Wabnitz, G. H., and Hänsch, G. M. (2016) Expression of the bitter receptor T2R38 in pancreatic cancer: localization in lipid droplets and activation by a bacteria-derived quorum-sensing molecule. *Oncotarget* **7,** 12623–12632 Medline
107. Wölfle, U., Elsholz, F. A., Kersten, A., Haarhaus, B., Schumacher, U., and Schempp, C. M. (2016) Expression and functional activity of the human bitter taste receptor TAS2R38 in human placental tissues and JEG-3 cells. *Molecules* **21,** 306 CrossRef Medline
108. Lee, R. J., and Foskett, J. K. (2010) cAMP-activated Ca^{2+} signaling is required for CFTR-mediated serous cell fluid secretion in porcine and human airways. *J. Clin. Invest.* **120,** 3137–3148 CrossRef Medline
109. Diggle, S. P., Lumjiaktase, P., Dipilato, F., Winzer, K., Kunakorn, M., Barrett, D. A., Chhabra, S. R., Cámara, M., and Williams, P. (2006) Functional genetic analysis reveals a 2-alkyl-4-quinolone signaling system in the human pathogen *Burkholderia pseudomallei* and related bacteria. *Chem. Biol.* **13,** 701–710 CrossRef Medline
110. Sisson, J. H., Pavlik, J. A., and Wyatt, T. A. (2009) Alcohol stimulates ciliary motility of isolated airway axonemes through a nitric oxide, cyclase, and cyclic nucleotide-dependent kinase mechanism. *Alcohol. Clin. Exp. Res.* **33,** 610–616 CrossRef Medline
111. Stout, S. L., Wyatt, T. A., Adams, J. J., and Sisson, J. H. (2007) Nitric oxide-dependent cilia regulatory enzyme localization in bovine bronchial epithelial cells. *J. Histochem. Cytochem.* **55,** 433–442 CrossRef Medline
112. Maniscalco, M., Sofia, M., and Pelaia, G. (2007) Nitric oxide in upper airways inflammatory diseases. *Inflamm. Res.* **56,** 58–69 CrossRef Medline
113. Sisson, J. H., May, K., and Wyatt, T. A. (1999) Nitric oxide-dependent ethanol stimulation of ciliary motility is linked to cAMP-dependent protein kinase (PKA) activation in bovine bronchial epithelium. *Alcohol. Clin. Exp. Res.* **23,** 1528–1533 Medline
114. Robbins, R. A., Sisson, J. H., Springall, D. R., Nelson, K. J., Taylor, J. A., Mason, N. A., Polak, J. M., and Townley, R. G. (1997) Human lung mononuclear cells induce nitric oxide synthase in murine airway epithelial cells *in vitro*: role of TNFα and IL-1β. *Am. J. Respir. Crit. Care Med.* **155,** 268–273 CrossRef Medline
115. Jain, B., Rubinstein, I., Robbins, R. A., and Sisson, J. H. (1995) TNF-α and IL-1 β upregulate nitric oxide-dependent ciliary motility in bovine airway epithelium. *Am. J. Physiol.* **268,** L911–L917 Medline
116. Sisson, J. H. (1995) Ethanol stimulates apparent nitric oxide-dependent ciliary beat frequency in bovine airway epithelial cells. *Am. J. Physiol.* **268,** L596–L600 Medline
117. Holban, A. M., Bleotu, C., Chifiriuc, M. C., Bezirtzoglou, E., and Lazar, V. (2014) Role of *Pseudomonas aeruginosa* quorum sensing (QS) molecules on the viability and cytokine profile of human mesenchymal stem cells. *Virulence* **5,** 303–310 CrossRef Medline
118. Hänsch, G. M., Prior, B., Brenner-Weiss, G., Obst, U., and Overhage, J. (2014) The *Pseudomonas* quinolone signal (PQS) stimulates chemotaxis of polymorphonuclear neutrophils. *J. Appl. Biomater. Funct. Mater.* **12,** 21–26 Medline
119. Tashiro, Y., Yawata, Y., Toyofuku, M., Uchiyama, H., and Nomura, N. (2013) Interspecies interaction between *Pseudomonas aeruginosa* and other microorganisms. *Microbes Environ.* **28,** 13–24 CrossRef Medline
120. Schuster, M., and Greenberg, E. P. (2006) A network of networks: quorum-sensing gene regulation in Pseudomonas aeruginosa. *Int. J. Med. Microbiol.* **296,** 73–81 CrossRef Medline
121. Gallagher, L. A., McKnight, S. L., Kuznetsova, M. S., Pesci, E. C., and Manoil, C. (2002) Functions required for extracellular quinolone signaling by *Pseudomonas aeruginosa*. *J. Bacteriol.* **184,** 6472–6480 CrossRef Medline
122. Wade, D. S., Calfee, M. W., Rocha, E. R., Ling, E. A., Engstrom, E., Coleman, J. P., and Pesci, E. C. (2005) Regulation of *Pseudomonas* quinolone signal synthesis in *Pseudomonas aeruginosa*. *J. Bacteriol.* **187,** 4372–4380 CrossRef Medline
123. Ferré, S. (2015) The GPCR heterotetramer: challenging classical pharmacology. *Trends Pharmacol. Sci.* **36,** 145–152 CrossRef Medline
124. Gahbauer, S., and Böckmann, R. A. (2016) Membrane-mediated oligomerization of G protein coupled receptors and its implications for GPCR function. *Front. Physiol.* **7,** 494 Medline
125. Kuhn, C., and Meyerhof, W. (2013) Oligomerization of sweet and bitter taste receptors. *Methods Cell Biol.* **117,** 229–242 CrossRef Medline
126. Kuhn, C., Bufe, B., Batram, C., and Meyerhof, W. (2010) Oligomerization of TAS2R bitter taste receptors. *Chem. Senses* **35,** 395–406 CrossRef Medline
127. Lee, R. J., Workman, A. D., Carey, R. M., Chen, B., Rosen, P. L., Doghramji, L., Adappa, N. D., Palmer, J. N., Kennedy, D. W., and Cohen, N. A. (2016) Fungal aflatoxins reduce respiratory mucosal ciliary function. *Sci. Rep.* **6,** 33221 CrossRef Medline
128. Jiang, P., Cui, M., Zhao, B., Snyder, L. A., Benard, L. M., Osman, R., Max, M., and Margolskee, R. F. (2005) Identification of the cyclamate interaction site within the transmembrane domain of the human sweet taste receptor subunit T1R3. *J. Biol. Chem.* **280,** 34296–34305 CrossRef Medline
129. Edelstein, A., Amodaj, N., Hoover, K., Vale, R., and Stuurman, N. (2010) Computer control of microscopes using microManager. *Curr. Protoc. Mol. Biol.* Chapter 14, Unit 14.20 CrossRef
130. Lai, Y., Chen, B., Shi, J., Palmer, J. N., Kennedy, D. W., and Cohen, N. A. (2011) Inflammation-mediated upregulation of centrosomal protein 110, a negative modulator of ciliogenesis, in patients with chronic rhinosinusitis. *J. Allergy Clin. Immunol.* **128,** 1207–1215.e1 CrossRef Medline
131. Zhao, K. Q., Cowan, A. T., Lee, R. J., Goldstein, N., Droguett, K., Chen, B., Zheng, C., Villalon, M., Palmer, J. N., Kreindler, J. L., and Cohen, N. A. (2012) Molecular modulation of airway epithelial ciliary response to sneezing. *FASEB J.* **26,** 3178–3187 CrossRef Medline
132. Lee, R. J., and Foskett, J. K. (2010) Mechanisms of Ca^{2+}-stimulated fluid secretion by porcine bronchial submucosal gland serous acinar cells. *Am. J. Physiol. Lung Cell Mol. Physiol.* **298,** L210–L231 CrossRef Medline
133. Lee, R. J., Limberis, M. P., Hennessy, M. F., Wilson, J. M., and Foskett, J. K. (2007) Optical imaging of Ca^{2+}-evoked fluid secretion by murine nasal submucosal gland serous acinar cells. *J. Physiol.* **582,** 1099–1124 CrossRef Medline
134. McMahon, D. B., Workman, A. D., Kohanski, M. A., Carey, R. M., Freund, J. R., Hariri, B. M., Chen, B., Doghramji, L. J., Adappa, N. D., Palmer, J. N., Kennedy, D. W., and Lee, R. J. (2018) Protease-activated receptor 2 activates airway apical membrane chloride permeability and increases ciliary beating. *FASEB J.* **32,** 155–167 CrossRef Medline
135. Fowler, C. J., and Tiger, G. (1997) Calibration of Fura-2 signals introduces errors into measurement of thrombin-stimulated calcium mobilisation in human platelets. *Clin. Chim. Acta* **265,** 247–261 CrossRef Medline
136. Shaul, P. W. (2002) Regulation of endothelial nitric oxide synthase: location, location, location. *Annu. Rev. Physiol.* **64,** 749–774 CrossRef Medline
137. Doerner, J. F., Delling, M., and Clapham, D. E. (2015) Ion channels and calcium signaling in motile cilia. *Elife* **4,** e11066 Medline
138. Lin, S., Fagan, K. A., Li, K. X., Shaul, P. W., Cooper, D. M., and Rodman, D. M. (2000) Sustained endothelial nitric-oxide synthase activation requires capacitative Ca^{2+} entry. *J. Biol. Chem.* **275,** 17979–17985 CrossRef Medline
139. Schindelin, J., Arganda-Carreras, I., Frise, E., Kaynig, V., Longair, M., Pietzsch, T., Preibisch, S., Rueden, C., Saalfeld, S., Schmid, B., Tinevez, J. Y., White, D. J., Hartenstein, V., Eliceiri, K., Tomancak, P., and Cardona, A. (2012) Fiji: an open-source platform for biological-image analysis. *Nat. Methods* **9,** 676–682 CrossRef Medline